N–H Activation by Rh(I) via Metal–Ligand Cooperation

ARTICLE *in* ORGANOMETALLICS · MAY 2012

Impact Factor: 4.13 · DOI: 10.1021/om300248r

5 AUTHORS, INCLUDING:

Yael Diskin-Posner
Weizmann Institute of Science
81 PUBLICATIONS **1,683** CITATIONS
SEE PROFILE

Linda J.W. Shimon
Weizmann Institute of Science
209 PUBLICATIONS **6,144** CITATIONS
SEE PROFILE

ORGANOMETALLICS

Article

pubs.acs.org/Organometallics

N−H Activation by Rh(I) via Metal−Ligand Cooperation

Moran Feller,[†] Yael Diskin-Posner,[‡] Linda J. W. Shimon,[‡] Eyal Ben-Ari,[†] and David Milstein*[,†]

[†]Department of Organic Chemistry and [‡]Department of Chemical Research Support, The Weizmann Institute of Science, Rehovot, 76100, Israel

Supporting Information

ABSTRACT: In continuation of our studies on bond activation and catalysis by pincer complexes, based on metal−ligand cooperation, we present here a rare example of amine N−H activation by Rh(I) complexes. The novel dearomatized pincer complexes [(PNN*)RhL′] (PNN = 2-(CH_2-P^{t}Bu$_2$)-6-(CH_2-NEt$_2$)C_5H_3N, PNN* = deprotonated PNN, L′ = N_2 (**5**), C_2H_4 (**6**)) and [(^{i}PrPNP*)RhL′] (^{i}PrPNP = 2,6-(CH_2-P^{i}Pr$_2$)$_2C_5H_3N$, ^{i}PrPNP* = deprotonated ^{i}PrPNP, L′ = C_2H_4 (**7**), cyclooctene (**9**)) were prepared and fully characterized by NMR and X-ray analysis. Complexes **5**−**7** and **9** undergo facile N−H activation of anilines involving aromatization of the pincer ligand without a change in the formal oxidation state of the metal center to form stable anilide complexes [(PNN)Rh(NHAr)] and [(^{i}PrPNP)Rh(NHAr)] (Ar = C_6H_5, *o*-Br-C_6H_4, *m*-Cl-*p*-Cl-C_6H_3, *p*-NO_2-C_6H_4). Anilines possessing electron-withdrawing groups accelerate the N−H activation and yield more stable anilide complexes. The pincer and the ancillary ligands also affect the activation rate, which supports an associative mechanism. Spin saturation transfer experiments show chemical exchange between the pyridylic arm of the pincer ligand and the NH− protons of anilines prior to and after the N−H activation. The reverse N−H formation by metal−ligand cooperation from the anilide complexes was observed to give free anilines and dearomatized Rh(I) complexes upon addition of CO or PEt_3. Deprotonation of complexes [(PNL)Rh(*p*-NO_2-$NH_2C_6H_4$)] (**13**, P = P^{t}Bu$_2$, L = NEt$_2$; **15**, P = L = P^{i}Pr$_2$) yields the dearomatized anionic complexes [(PNL*)Rh(*p*-NO_2-$NH_2C_6H_4$)]. An associative mechanism, involving N−H activation of an apically coordinated aniline in a pentacoordinated Rh(I) complex, is suggested.

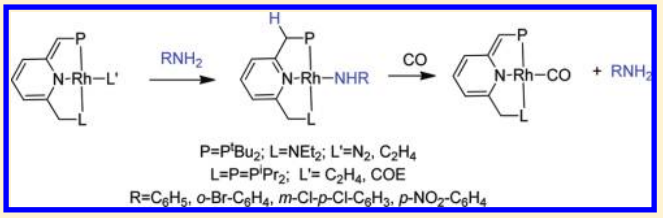

INTRODUCTION

Our group has discovered a new mode of metal−ligand cooperation, involving aromatization−dearomatization of pyridine-based ^{R}PNP and PNN (R = ^{t}Bu; ^{i}Pr) pincer ligands (Scheme 1), as well as bipyridine-based PNN pincer ligands. Metal−ligand cooperation based on acridine pincer complexes has also been demonstrated.[1]

Scheme 1

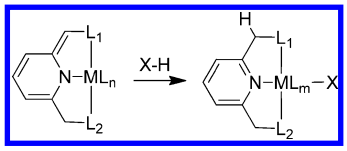

Metal−ligand cooperation by aromatization−dearomatization is involved in several new, environmentally benign reactions developed by us, catalyzed by pincer-type PNN-Ru,[2,3] PNP-Ru,[2a,h,4] acridine-PNP-Ru,[5] and PNP-Fe[6] complexes, including (a) dehydrogenative coupling of primary alcohols to form esters,[2a,d,h,4a] (b) dehydrogenation of secondary alcohols to ketones,[2b,h,4a] (c) hydrogenation of esters to alcohols[2c,h,7] and cyclic diesters to diols,[3c] (d) coupling of alcohols with amines to form amides with liberation of H_2,[2d] (e) formation of polyamides by dehydrogenative coupling of diamines and diols,[2i,8] (f) hydrogenation of amides to amines and alcohols,[3a] (g) dehydrogenative acylation of alcohols with esters,[2e] (h) dehydrogenative amidation of esters with amines,[2f] (i) hydrogenation of organic carbonates, carbamates, and formate esters, indicating a mild, two-step hydrogenation of CO_2 to methanol,[2g] (j) hydrogenation of urea derivatives to form methanol and amines,[3b] (k) selective formation of primary amines from alcohols and ammonia, with liberation of water,[5c] (l) dehydrogenative coupling of primary alcohols to form acetals,[5b] (m) coupling of *β*-amino alcohols to form peptides by PNN-Ru, or pyrazines by PNP-Ru, with H_2 liberation,[9] (n) Fe-catalyzed hydrogenation of ketones at low pressure and ambient temperature,[6a,c] (o) Fe-catalyzed hydrogenation of CO_2 to formate salts at low pressure[6b] and (p) direct synthesis of imines from alcohols and amines with liberation of H_2 and water.[4b] Polymerization of diols to form polyesters with H_2 liberation catalyzed by the PNN-Ru complex was also reported.[10] Several computational studies (DFT) of these catalytic reactions have appeared.[11]

Other examples of bond activation and catalysis that involve (or may involve) metal ligand cooperation by aromatization−dearomatization of pyridine-based pincer complexes were recently reported.[12]

The activation of X−H (X = H, C, O, N) bonds via metal−ligand cooperation by aromatization−dearomatization of the

Received: May 7, 2012
Published: May 18, 2012

   dx.doi.org/10.1021/om300248r | *Organometallics* 2012, 31, 4083−4101

ligand formally involves proton transfer from a substrate to the dearomatized ligand, which leads to H−X cleavage with concomitant aromatization and no change in the oxidation state of the metal center. The activation of Csp^2−H and Csp^3−H bonds was demonstrated by the dearomatized pincer complex [(^{t}BuPNP*)Ir(COE)], which reacts with benzene[13a] and acetone[13b] to give the aromatic complexes [(^{t}BuPNP)Ir(R)] (R = C_6H_5 and CH_2COCH_3, respectively), with no overall change in the formal metal oxidation state (Scheme 2).

Scheme 2

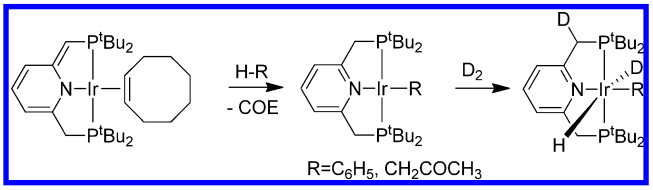

The latter complexes react with H_2 to give exclusively the *trans*-dihydride complexes, and upon reaction with D_2, the *trans*-hydride−deuteride complexes [(^{t}BuPNP)Ir(H)(D)(R)], with one deuterium atom incorporated into a benzylic position, are obtained (Scheme 2).[13] The complex that activates H_2 was found to be an Ir(III) intermediate [(^{t}BuPNP*)Ir(H)(R)], which is in equilibrium with the Ir(I) complex [(^{t}BuPNP)Ir(R)].[13,14] The anionic dearomatized pincer complex [(^{t}BuPNP*)RhCl][K] activates benzene and hydrogen by metal−ligand cooperation to yield the corresponding aromatized phenyl and hydrido complexes, respectively.[15]

The complex [(PNN*)RuH(CO)], bearing a dearomatized pincer ligand, activates O−H bonds of alcohols[2] and water.[16] The reaction with water yields the aromatized *trans*-hydrido−hydroxo complex [(PNN)Ru(H)(CO)(OH)]. The latter promotes water splitting to H_2 and O_2 in a stoichiometric cycle involving consecutive heat- and light-induced steps, using no sacrificial reagents.[16] Here, we focus on the activation of N−H bonds of amines by pincer complexes based on metal−ligand cooperation.

Amines are an important class of compounds with a wide range of uses in the chemical, pharmaceutical, and agrochemical industries, as intermediates, surfactants, dyes, polymers, plasticizing agents, and fine chemicals.[17] N−H bond activation and N−H elimination of amines mediated by metal complexes could be fundamental steps in the catalytic formation and functionalization of amines, although examples of such processes are rare and far less explored than the activation of C−H and O−H bonds. Investigation of N−H bond activation and formation can also shed light on important metal-catalyzed transformations, which involve amines and ammonia,[18] such as hydroamination,[19] hydroaminomethylation,[20] aryl halides amination,[21] reductive aminations,[22] and reduction of nitriles.[23]

The first example of catalytic olefin amination based on N−H activation was demonstrated by our group using an Ir(I) complex.[24]

The few reported direct observations of N−H oxidative addition of amines by late transition metals include the early example of aniline activation by $Ru_3(CO)_{12}$,[25] N−H oxidative addition of indoles by [Ir(COD)(PMe_3)$_3$][Cl],[26] and aniline oxidative addition by (PCP)Ir[27] and (POCOP)Ir[28] complexes (PCP = 2,6-(CH_2-P^{t}Bu$_2$)$_2$$C_6H_3$, POCOP = 2,6-(OP^{t}Bu$_2$)$_2$$C_6H_3$) to give anilido hydride complexes.[29] Direct observation of oxidative addition of ammonia to Ir(I), to form amido-bridged iridium hydride dimers, was reported by our group.[30] Hartwig and Goldman reported ammonia oxidative addition by the pincer complex [^{t}Bu$_2$P(CH_2)$_2$CH-(CH_2)$_2$P^{t}Bu$_2$]Ir(I), to form a monomeric amido iridium hydride.[31] Hartwig also reported the double N−H cleavage of hydrazines by pincer Ir complexes.[32] Turculet reported the N−H oxidative addition of ammonia and anilines by an iridium silyl pincer complex to give stable anilido hydride complexes [(Cy-PS^{i}P)Ir(H)(NHR)] (Cy-PS^{i}P = MeSi(*o*-C_6H_4PCy$_2$)$_2$).[33] The corresponding Rh silyl complex reacts with anilines and ammonia to give only adduct complexes. Activation of ammonia by a dimeric Pd pincer complex via a binuclear oxidative addition to give amido and hydrido Pd monomers was described by Ozerov and co-workers.[34] Very recently, Oro has reported formation of M-NH_2 (M = Rh, Ir) by reaction of ammonia with {M(μ-OMe)(tetrafluorobenzobarrelene)}$_2$.[35]

Recently, we have reported N−H activation of amines promoted by the nonaromatic complex [(^{t}BuPNP*)RuH(CO)] via metal−ligand cooperation.[36] The reaction of this complex with electron-rich amines, such as ammonia, leads to reversible activation, while with electron-poor substrates, such as *p*-nitroaniline, stable N−H activation products are obtained (Scheme 3). N−H activation of amides (rather than amines) by metal−ligand cooperation was very recently reported by Muniz.[37]

Scheme 3

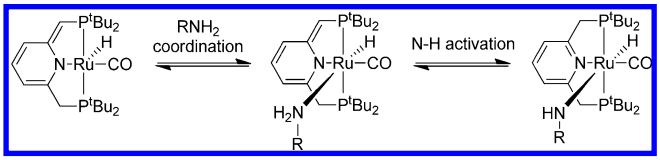

Here, we report on a rare case of N−H activation via metal−ligand cooperation by novel dearomatized ^{i}PrPNP- and PNN-based Rh(I) complexes. The obtained anilido complexes react with ancillary ligands, such as CO, to eliminate anilines via metal−ligand cooperation, regaining dearomatization. Mechanistic issues of this unusual N−H activation process are discussed.

RESULTS AND DISCUSSION

Synthesis and Characterization of PNN and ^{i}PrPNP Rh(I) Complexes. Addition of the PNN ligand (PNN = 2-(CH_2-P^{t}Bu$_2$)-6-(CH_2-NEt$_2$)C_5H_3N) to a THF solution of the cationic precursor [Rh(COE)$_2$(THF)$_2$][BF_4] (COE = cyclooctene) under nitrogen resulted in the formation of a yellow precipitate that was isolated and characterized as the cationic dinitrogen complex [(PNN)RhN_2][BF_4] (**1**) (Scheme 4). The $^{31}P\{^1H\}$ NMR spectrum of **1** exhibits a sharp doublet at 93.31 ppm ($^1J_{RhP}$ = 161.6 Hz) both in acetone and in methylene chloride.[38] The ^{19}F NMR spectrum of complex **1** in acetone exhibits a sharp signal at −152 ppm, typical of a free BF_4 counteranion, while the ^{19}F NMR spectrum recorded in methylene chloride[39] exhibits a very broad signal at −151.5 ppm, which becomes narrower at lower temperatures.[40,41] Thus, in the noncoordinating methylene chloride solvent, a weak interaction of the metal center with the counterion is observed at ambient temperature.[41a,42] This weak metal−counteranion interaction probably stabilizes the complex, whereas in acetone, stabilization is gained by solvent coordination.

dx.doi.org/10.1021/om300248r | *Organometallics* 2012, 31, 4083−4101

Scheme 4

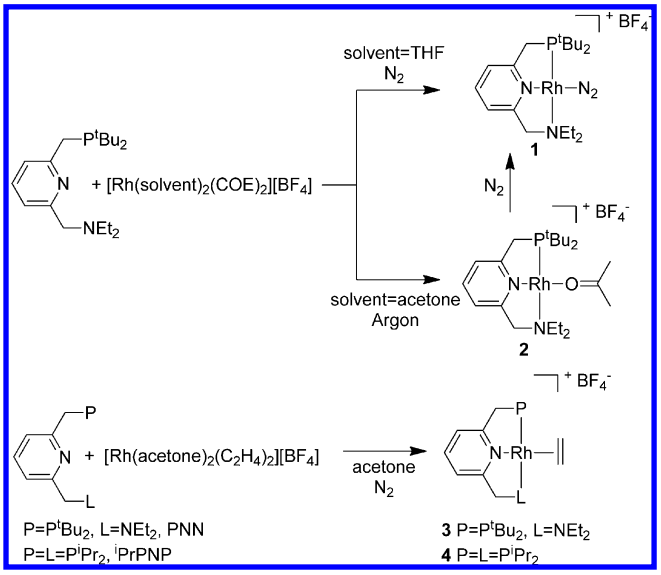

As mentioned above, complex **1** was characterized as a mononuclear "end-on" N_2 complex under nitrogen; however, when a concentrated acetone solution of **1** was layered with pentane, crystals of the N_2-bridged dimeric complex $[(PNN)Rh]_2(N_2\text{-}\mu)[2BF_4]$ (**1a**) were obtained (Figure 1, Table 1). The

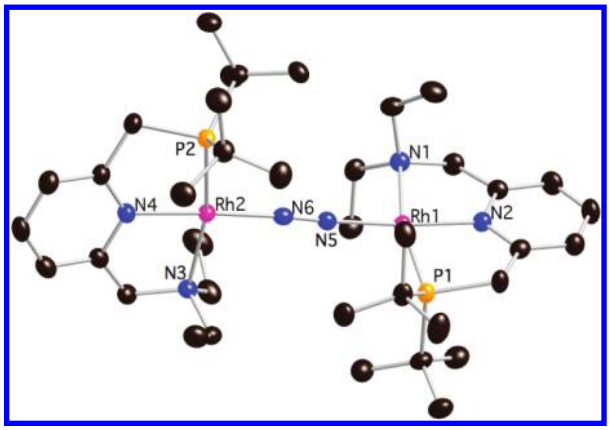

Figure 1. X-ray crystal structure of **1a** at the 50% probability level. Hydrogen atoms and counteranions are omitted for clarity.

Table 1. Selected Bond Lengths (Å) and Bond Angles (deg) of 1a

Rh(1)−N(1)	2.168(2)	N(2)−Rh(1)−N(5)	174.86(9)
Rh(1)−N(2)	2.007(2)	N(1)−Rh(1)−P(1)	164.98(6)
Rh(1)−N(5)	1.913(2)	Rh(1)−N(5)−N(6)	176.8(2)
Rh(1)−P(1)	2.2342(7)	N(4)−Rh(2)−N(6)	176.75(9)
Rh(2)−N(3)	2.175(2)	N(3)−Rh(2)−P(2)	165.67(6)
Rh(2)−N(4)	2.008(2)	Rh(2)−N(6)−N(5)	175.5(2)
Rh(2)−N(6)	1.922(2)		
Rh(2)−P(2)	2.2412(7)		
N(5)−N(6)	1.124(3)		

X-ray structure of **1a** reveals a binuclear complex with a distorted square-planar geometry around the metal centers. The planes of the two pyridine rings are almost perpendicular, with a dihedral angle of 79°. The N(5)−N(6) bond length is longer by 0.03 Å than in free dinitrogen, as expected for a bridging N−N bond.[43]

Addition of the PNN ligand to an acetone solution of the cationic precursor $[Rh(COE)_2(acetone)_2][BF_4]$ under argon resulted in the formation of the cationic complex **2** (Scheme 4).[44] The $^{31}P\{^1H\}$NMR spectrum of **2** reveals a sharp doublet at 86.85 ppm ($^1J_{RhP}$ = 193.4 Hz). The X-ray crystal structure of **2** (Figure 2, Table 2) exhibits a distorted square-planar geometry with N(1)−Rh(1)−P(1) and N(2)−Rh(1)−O(1) bond angles of 163.9° and 176.1°, respectively. The bond angle Rh(1)−O(1)−C(20) of 132.1° indicates that the acetone ligand is coordinated through one of the oxygen electron lone pairs. The ^{19}F NMR of **2** reveals a broad signal at 151.5 ppm, implying a weak interaction of the counteranion with the metal center in the solution.[42] When complex **2** was exposed to a nitrogen atmosphere, the dinitrogen complex **1** was formed.

Complexes **3** and **4** were obtained by addition of the ligands PNN and ^{i}PrPNP (^{i}PrPNP = 2,6-$(CH_2\text{-}P^iPr_2)_2C_5H_3N$), respectively, to an acetone solution of $[Rh(C_2H_4)_2(acetone)_2]$-$[BF_4]$ under nitrogen. The $^{31}P\{^1H\}$ NMR spectra of **3** and **4** exhibit sharp doublets at 81.65 ppm ($^1J_{RhP}$ = 168.9 Hz) and 53.90 ($^1J_{RhP}$ = 122.4 Hz), respectively. The ethylene ligands of **3** and **4** give rise to a signal at 3.50 ppm in the ^1H NMR spectrum, as in the case of the analogous complex $[(^t$BuPNP)-$Rh(C_2H_4)][OTf]$,[45] and about 2 ppm upfield from the chemical shift of free ethylene. The ethylene ligand of **3** appears as a broad singlet,[46] whereas that of **4** exhibits a sharp triplet of doublets signal ($^3J_{PH}$ = 3.3 Hz, $^2J_{RhH}$ = 2.2 Hz). In the $^{13}C\{^1H\}$ NMR spectrum, the ethylene ligands of **3** and **4** appear as a doublet at 59.72 ppm ($^1J_{CRh}$ = 12.7 Hz) and as a doublets of triplet at 52.34 ($^1J_{RhC}$ = 10.7 Hz, $^2J_{PC}$ = 1.7 Hz), respectively, about 60−65 ppm upfield from the free ethylene signal. The X-ray structures of **3** and **4** reveal distorted square-planar geometries around the metal center (Figure 2, Table 3)[47] with ethylene bonds (C(20)−C(21)) slightly elongated as compared with free ethylene.[48]

Synthesis and Characterization of Dearomatized (PNN) and (^{i}PrPNP) Rh(I) Complexes. Upon reaction of complex **1** with an equivalent of base (^{t}BuOK) in THF, a mixture of the neutral, dearomatized dinitrogen mononuclear and dinuclear complexes **5** and **5a**, respectively, was obtained (Scheme 5). According to the $^{31}P\{^1H\}$ NMR spectrum at 297 K, the mononuclear form is the dominant one, with a molar ratio of **5**:**5a** = 3:1, whereas at 215 K, the ratio is **5**:**5a** = 2:1.

Complexes **3**, **4**, and the previously reported complex $[(^i$PrPNP)Rh(COE)][BF_4][49] (**8**) also afforded the dearomatized complexes **6**, **7**, and **9**, respectively, by deprotonation in quantitative yields (Scheme 5). The $^{31}P\{^1H\}$ NMR spectra of **5**, **5a**, and **6** give rise to sharp doublets at 84.76 ($^1J_{RhP}$ = 173.7 Hz), 83.51 ($^1J_{RhP}$ = 170.1 Hz), and 70.71 ($^2J_{RhP}$ = 177.4 Hz) ppm, respectively, shifted about 10 ppm upfield as compared with the cationic analogues. In addition, the Rh−P coupling constants are increased by about 8 Hz, which may imply a stronger Rh−P σ bond in the dearomatized complexes. The ^1H NMR spectra of **5** and **6** give rise to a signal at 3.4 ppm corresponding to one proton, which give a ^1J C−H correlation with a CH doublet signal at 62.7 ppm ($^1J_{PC}$ = 57.1 Hz) and 67.39 ppm ($^1J_{PC}$ = 55.2 Hz), respectively, indicating that deprotonation at the benzylic phosphine "arm" took place. Moreover, the benzylic amine "arm" gives rise to a two-proton singlet in the ^1H NMR spectrum at 3.13 and 2.89 ppm for complexes **5** and **6**, respectively, about 1.5 ppm upfield shifted in comparison with the cationic complexes **1** and **3**. These

dx.doi.org/10.1021/om300248r | Organometallics 2012, 31, 4083−4101

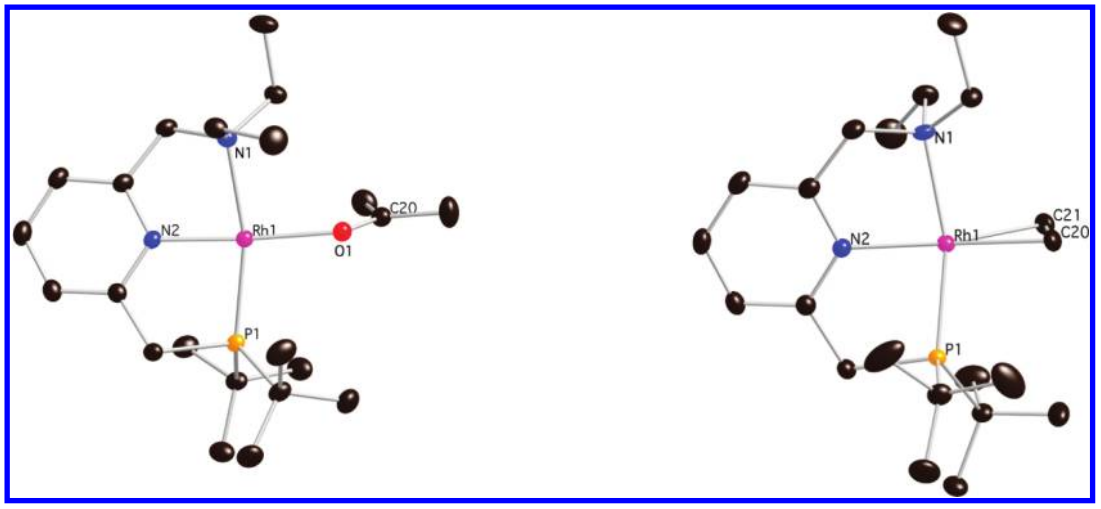

Figure 2. X-ray crystal structure of **2** (left) and **3** (right) at the 50% probability level. Hydrogen atoms and counteranions are omitted for clarity.

Table 2. Selected Bond Lengths (Å) and Bond Angles (deg) of 2

Rh(1)−N(1)	2.1906(14)	N(1)−Rh(1)−P(1)	163.90(4)
Rh(1)−N(2)	1.9660(13)	N(2)−Rh(1)−O(1)	176.13(5)
Rh(1)−P(1)	2.2167(4)	N(1)−Rh(1)−N(2)	80.56(5)
Rh(1)−O(1)	2.0839(12)	P(1)−Rh(1)−N(2)	84.54(4)
O(1)−C(20)	1.235(2)	N(1)−Rh(1)−O(1)	95.65(5)
		P(1)−Rh(1)−O(1)	99.15(4)
		Rh(1)−O(1)−C(20)	132.07(12)

Table 3. Selected Bond Lengths (Å) and Bond Angles (deg) of 3 and 4

	[(PNN)Rh(C_2H_4)][BF_4] (**3**)	[(^{i}PrPNP)Rh(C_2H_4)][BF_4] (**4**)
Rh(1)−N(1)	2.2205(17)	
Rh(1)−N(2)	2.0504(17)	2.101(2)
Rh(1)−P(1)	2.2385(5)	2.2872(7)
Rh(1)−P(2)		2.2831(7)
Rh(1)−C(20)	2.150(2)	2.123(3)
Rh(1)−C(21)	2.139(2)	2.131(3)
C(20)−C(21)	1.376(4)	1.334(6)
N(1)−Rh(1)−P(1)	163.72(5)	
N(1)−Rh(1)−N(2)	81.03(7)	
P(1)−Rh(1)−N(2)	83.13(5)	83.68(6)
N(2)−Rh(1)−C(20)	164.69(9)	161.74(16)
N(2)−Rh(1)−C(21)	157.41(9)	161.73(15)
P(2)−Rh(1)−N(2)		84.30(6)
P(1)−Rh(1)−P(2)		167.95(2)

signals give a ^1J C−H correlation with a CH_2 doublet signal at 63 ppm[50] (d, J = 1.8 Hz) and 64.07 ppm (d, J = 1.5 Hz), respectively, about the same chemical shift as in the starting cationic complexes.

Complex **7** exhibits an AB splitting pattern, indicating two nonequivalent phosphine atoms. The deprotonated "arm" of **7** gives rise to a doublet signal at 3.35 ppm ($^2J_{PH}$ = 4.0 Hz) in the ^{1}H NMR spectrum, corresponding to one proton, and a CH doublet signal at 63.36 ($^1J_{PC}$ = 50.8 Hz) in the $^{13}C\{^1H\}$ DEPT spectra. The $^{31}P\{^1H\}$ NMR spectrum of complex **9** exhibits very broad signals at ambient temperature, and a sharp AB system at 223 K centered at 32.63 (dd, $^1J_{RhP}$ = 136.2 Hz, $^2J_{PP}$ = 312.8 Hz) and 45.55 (dd, $^1J_{RhP}$ = 130.4 Hz, $^2J_{PP}$ = 312.8 Hz). We assume that the fluxionality of complex **9** is due to weak coordination of the bulky COE ligand. Indeed, when an excess of ethylene was introduced to a benzene solution of complex **9**, the ethylene complex **7** was obtained. On the other hand, complex **7** did not react with a large excess of COE.

The N−N IR band of complex **5** (2110 cm^{-1}) is slightly red shifted from one of the two N−N stretching frequencies of **1** (2157 cm^{-1}). A similar shift was observed for the [(^{t}BuPNP*)-RhN_2] complex.[51] The ethylene ligands in complexes **6** and **7** exhibit an upfield shift of 0.64 and 0.30 ppm in the ^{1}H NMR spectra and 16.29 and 7.83 ppm in the $^{13}C\{^1H\}$ NMR spectra, respectively, as compared with their cationic analogous **3** and **4**, suggesting an enhancement of the π-back-donation due to deprotonation.

Deprotonation of complex **2** under argon was not selective and resulted in a mixture of four unidentified complexes.

N−H Activation of Anilines by Dearomatized (PNN) and (^{i}PrPNP) Rh(I) Complexes. *Synthesis and Characterization of the Resulting Anilide Complexes.* Interestingly, upon reaction of the dearomatized PNN and ^{i}PrPNP Rh(I) complexes **5**[52]−**7** and **9** with an equivalent of aniline or substituted aniline at 60 °C, N−H activation took place, resulting in aromatization of the pincer ligand and formation of stable Rh(I) anilide complexes (Scheme 6). The $^{31}P\{^1H\}$NMR spectra of the PNN anilide complexes **10**−**13** feature a sharp doublet at 87 ppm with a $^1J_{RhP}$ coupling constant of 206−220 Hz, which is larger than that observed for the Rh(I) cationic or dearomatized complexes **1**−**3** and **5**−**6** ($^1J_{RhP}$ = 160−180 Hz). The $^{31}P\{^1H\}$NMR spectra of the ^{i}PrPNP anilide complexes **14** and **15** reveal only one doublet signal at about 45 ppm, indicating equivalent phosphines. The $^1J_{RhP}$ coupling constants of complexes **14** and **15** are also larger than in the case of complexes **4** and **7**−**9**. The ^{1}H NMR spectra of the PNN-based anilide complexes **10**−**13** exhibit two proton signals for the two benzylic "arms", and in complexes **14** and **15**, the phosphine benzylic "arms" give rise to a 4-proton virtual triplet signal. The NH-C anilide carbon is shifted to lower field by 10−15 ppm relative to the corresponding free aniline. However, the Rh−NHAr ^{1}H signals are shifted to higher field. For example, the Rh−NH signal in complexes **10** and **14** is shifted by 0.88 and 1.88 ppm, respectively, as compared with that in free aniline.

Crystallographic characterization of **12** confirmed the formation of an aromatic anilide complex and revealed a

dx.doi.org/10.1021/om300248r | *Organometallics* 2012, 31, 4083−4101

Scheme 5

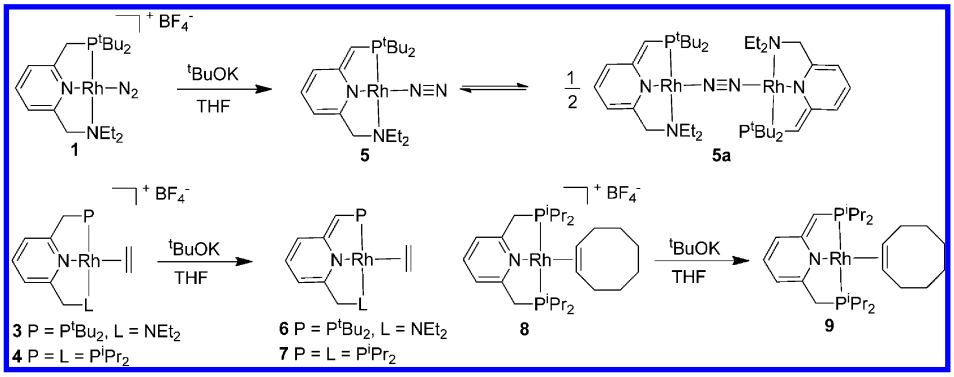

Scheme 6

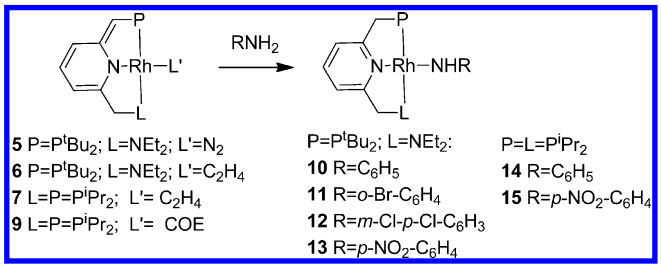

slightly distorted square-planar geometry (P(1)−Rh(1)−N(2) = 165.05(11)°) with an amide ligand positioned trans to an aromatic pyridine moiety (Figure 3, Table 4). The anilide aryl

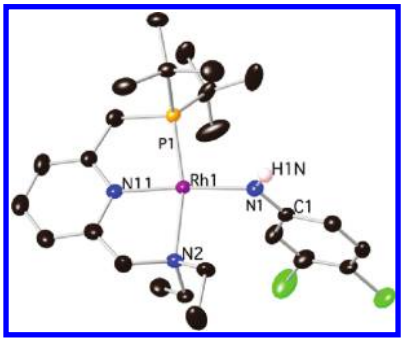

Figure 3. X-ray crystal structure of **12** at the 50% probability level. Hydrogen atoms (besides N(1)-H) are omitted for clarity.

Table 4. Selected Bond Lengths (Å) and Bond Angles (deg) of 12[a]

Rh(1)−N(1)	2.063(3)	P(1)−Rh(1)−N(2)	165.05(11)
Rh(1)−N(2)	2.243(4)	N(1)−Rh(1)−N(11)	175.30(12)
Rh(1)−N(11)	1.982(3)	N(11)−Rh(1)−N(2)	82.69(14)
Rh(1)−P(1)	2.1816(8)	P(1)−Rh(1)−N(11)	84.34(9)
N(1)−C(1)	1.353(4)	N(1)−Rh(1)−N(2)	92.60(14)
		N(1)−Rh(1)−P(1)	100.33(8)
		Rh(1)−N(1)−C(1)	129.1(3)

[a]Another conformer with a different position at N(2) was also detected.

and the pyridine planes are almost perpendicular with a dihedral angle of 83.9°. The Rh(1)−N(1) bond distance (2.063(3) Å) in **12** is comparable to that of other anilide late transition-metal complexes.[27,28,29a,33,53]

While the anilide ligand in complexes **10** and **14** retains its symmetry and exhibits only three CH signals in the ^{1}H and ^{13}C NMR spectra, the *p*-nitroanilide ligand in complexes **13** and **15** gives rise to four signals. The inequivalence of the two sides of the ring in complexes **13** and **15** indicates that the *p*-nitroanilide ligand is not rotating on the NMR time scale. However, the retained symmetry in the case of the anilide complexes **10** and **14** is probably not due to facile rotation, but rather to fast dissociation−association of aniline. Spin saturation transfer (SST) experiments[54] preformed with complexes **10**, **13**, **14**, and **15** support this assumption. Selective spin saturation of the Py−CH_2−P signal in complex **10** indicates a chemical exchange between the benzylic phosphine "arm" and the N−H anilide proton (Figure 4). Upon selective irradiation of the Py−CH_2−N signal, only negligible exchange between the benzylic amine "arm" and the N−H anilide proton was observed. Addition of an excess of aniline to a benzene solution of **10** and selective irradiation of the Py−CH_2−P signal revealed chemical exchange with the free aniline. SST experiments with complex **14** also demonstrated fast chemical exchange between the "benzylic arm" protons and the anilide ligand, both in the presence or in the absence of free aniline. In the presence of free aniline, exchange with the NH_2 group is also observed. In the case of the *p*-nitroanilide complexes **13** and **15**, no SST effect was observed, indicating that the N−H activation in this case is irreversible.

Complexes **10** and **14** can be obtained indirectly by deprotonation of the cationic aniline complexes **16** and **17**, respectively. Addition of excess aniline to THF suspensions of complexes **1** and **8** resulted in the cationic aniline complexes in high yield after heating to 60 °C for 2 and 4 h respectively. Complexes **16** and **17** were further reacted with ^{t}BuOK to give the anilide complexes **10** and **14** in 83% and 89% yields, respectively (Scheme 7). By contrast, addition of the less basic *p*-nitroaniline to the cationic complexes **1** and **8** did not yield the corresponding *p*-nitroaniline cationic PNN and ^{i}PrPNP complexes. Complexes **16** and **17** exhibit sharp doublet signals in the ^{31}P{^{1}H} NMR at 82.99 ($^{1}J_{RhP}$ = 197.1 Hz) and 49.29 ($^{1}J_{RhP}$ = 135.7 Hz), respectively. While the chemical shifts of the cationic aniline complexes **16** and **17** are only slightly shifted (by about 4 ppm) upfield as compared to their anilide analogues **10** and **14**, respectively, the $^{1}J_{RhP}$ coupling constants are dramatically decreased, by 23 and 21 Hz, respectively, and are in the range of cationic Rh(I) PNN and ^{i}PrPNP complexes. Complex **17** is a stable, isolable complex, in contrast to complex **16**, which was stable in solution only in the presence of an excess of aniline. This may be due to the steric hindrance imposed by the P^{t}Bu$_2$ group. The NMR spectrum of complex

dx.doi.org/10.1021/om300248r | *Organometallics* 2012, 31, 4083−4101

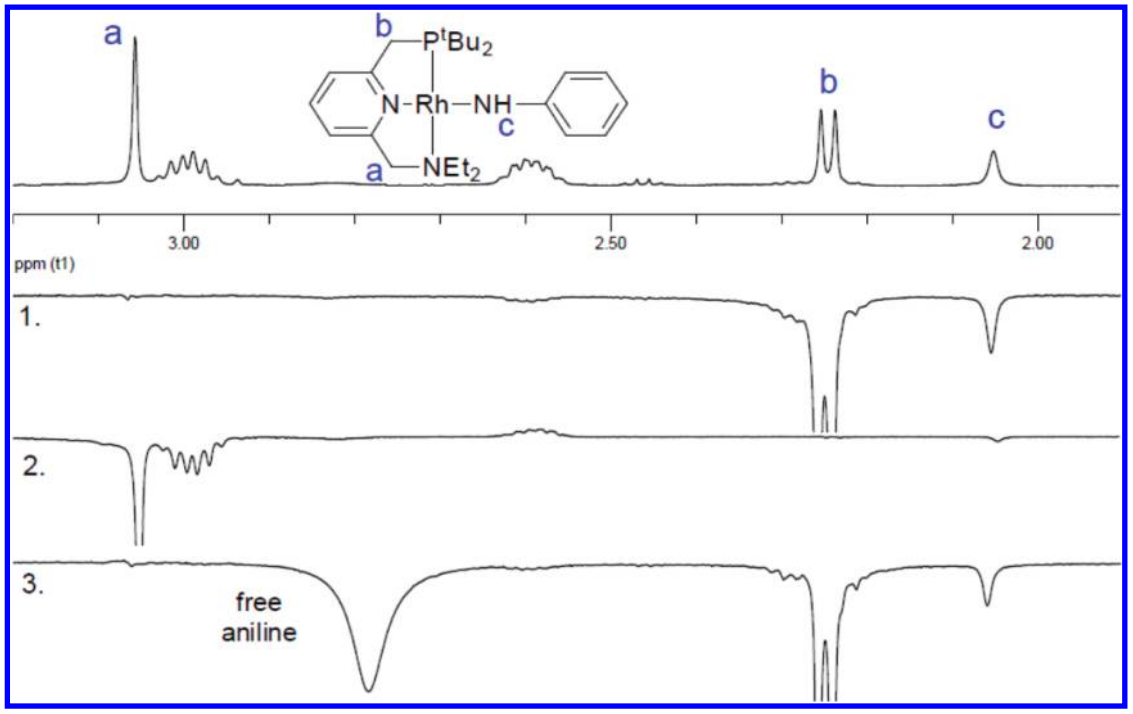

Figure 4. Spin saturation transfer experiments with complex **10**. Top view: ^{1}H NMR spectrum of **10** in benzene. (1 and 2): Spin saturation of signals b and a,[55] respectively, in the absence of free aniline. (3): Spin saturation of signal b in the presence of free aniline. (The multiplets at 2.6 and 3.0 ppm are assigned to N(CH_2CH$_3$).)

Scheme 7

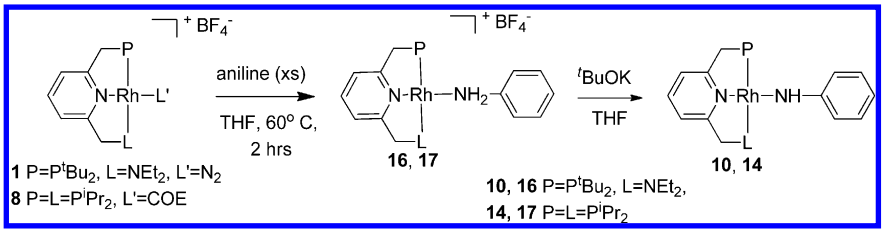

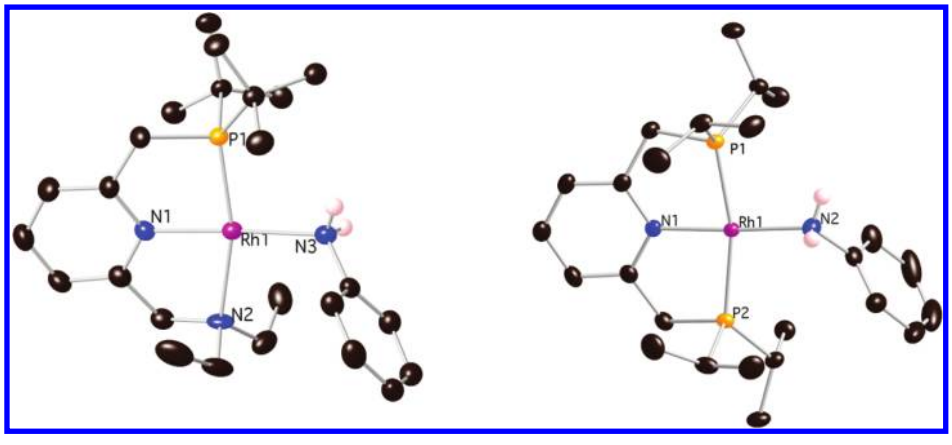

Figure 5. X-ray crystal structure of **16** (left) and **17** (right) at the 50% probability level. Hydrogen atoms (besides N(3)-H in **16** and N(2)-H in **17**) and counteranions are omitted for clarity.

16 exhibits separate signals of the bound and the free added aniline. The NH–*C* carbons of the aniline ligand are slightly shifted upfield in complexes **16** and **17** (by 4.7 and 1.1 ppm, respectively) relative to free aniline, and by about 16 ppm relative to the anilide ligand in complexes **10** and **14**. The Rh–N*H* signals of complexes **16** and **17** are shifted upfield by 0.57 and 0.91 ppm, respectively, as compared with the amino group of free aniline, in an opposite trend to the anilide complexes **10** and **14**. Single-crystal X-ray structures of **16** and **17** (Figure 5, Tables 5 and 6 respectively) reveal a slightly distorted square-planar geometry. The aniline and the pyridine planes are almost perpendicular with a dihedral angle of about 89° and 80° for **16** and **17**, respectively, as in complex **12**. The Rh–N(aniline) bond lengths in **16** and **17** are longer by about 0.085 and 0.07

dx.doi.org/10.1021/om300248r | *Organometallics* 2012, 31, 4083–4101

Table 5. Selected Bond Lengths (Å) and Bond Angles (deg) of 16[a]

Rh(1)−P(1)	2.2125(9)	P(1)−Rh(1)−N(2)	163.32(9)
Rh(1)−N(1)	1.998(3)	N(1)−Rh(1)−N(3)	176.91(12)
Rh(1)−N(2)	2.215(3)	N(1)−Rh(1)−P(1)	83.39(9)
Rh(1)−N(3)	2.143(3)	N(1)−Rh(1)−N(2)	81.00(12)
N(3)−C(20)	1.455(5)	N(3)−Rh(1)−P(1)	98.69(9)
		N(3)−Rh(1)−N(2)	97.15(12)
		Rh(1)−N(3)−C(20)	117.8(2)

[a]The X-ray structure of **16** contains two molecules of the complex in the asymmetric unit.

Table 6. Selected Bond Lengths (Å) and Bond Angles (deg) of 17

Rh(1)−P(1)	2.2691(5)	P(1)−Rh(1)−P(2)	165.717(18)
Rh(1)−P(2)	2.2943(5)	N(1)−Rh(1)−N(2)	176.99(6)
Rh(1)−N(1)	2.0618(15)	N(1)−Rh(1)−P(1)	83.99(4)
Rh(1)−N(2)	2.1299(16)	N(1)−Rh(1)−P(2)	83.14(4)
N(2)−C(20)	1.438(3)	N(2)−Rh(1)−P(1)	93.19(5)
		N(2)−Rh(1)−P(2)	99.54(5)
		Rh(1)−N(2)−C(20)	118.93(12)

Å, respectively, as compared with the corresponding bond of the anilide complex **12**.

Trends in Reactivity. The N−H activation process was faster with electron-poor anilines, such as *p*-nitroaniline, than with more basic anilines, such as aniline itself. For example, the reactions of the PNN complex **5** with an equivalent of aniline and *p*-nitroaniline at 60 °C reached completion after 9 and 5 h, respectively. Moreover, the reactions of complexes **5**−**7** and **9** with *p*-*tert*-butylaniline were sluggish and not selective. A similar trend was observed in the N−H activation of anilines by the complex [(PNN*)RuH(CO)], both experimentally and by DFT calculations.[36] The PNN* Ru complex gave stable anilide complexes only with the electron-poor anilines *p*-nitroaniline and *o*-chloro-*p*-nitroaniline, whereas with the halide-substituted anilines *o*-bromoaniline and *m*-chloro-*p*-chloroaniline, an equilibrium was observed. DFT studies show that the formation of electron-poor anilides is thermodynamically favorable by 10−15 kcal/mol. Brookhart and co-workers also observed a similar trend of reactivity with N−H oxidative addition to a 14-electron Ir(I) pincer complex.[28]

We have also examined the reactivity of the PNP complex [(^{t}BuPNP*)RhN$_2$][51] toward N−H activation and have found that the reactions were rather slow and nonselective. We believe that this is a result of steric hindrance of the bulkier PNP complex as compared with PNN complexes. In line with steric hindrance retardation of N−H activation, the reaction of complex **5** with the bulky 2,4,6-tribromoaniiline was nonselective and gave a mixture of four unidentified products.

The N−H activation rate was found to be affected by the aniline substituents, the pincer ligand, and the ancillary ligands. Follow-up of the progress of reactions of complexes **5**−**7** and **9** with an equivalent of *p*-nitroaniline using the same concentrations and temperatures[56] reveals that the rate of N−H activation follows the trend **7** > **9** > **5** > **6**. Thus, reaction of *p*-nitroaniline with complexes **5**, **7**, and **9** at 60 °C reached completion after 5 h, less than 5 and 25 min, respectively, whereas complex **6** reached 66% conversion after 24 h. Significantly, the reaction rate of complex **9** was accelerated in the presence of an excess (60 equiv) of COE, and the reaction reached completion after 5 min at ambient temperature instead of 5 h at the same conditions in the absence of added COE.

Follow-up of the progress of reactions of complexes **5**−**7** and **9** with an equivalent of aniline using the same concentrations and temperatures reveals that the rate of N−H activation follows the order **9** > **5** > **6** > **7**.[57] Thus, the reaction of complexes **5**−**7** and **9** with aniline under the same conditions and temperatures led to full conversion of complexes **9** and **5** after 6 and 7 h, respectively, whereas only 60% and 10% conversions were observed for complexes **6** and **7**, respectively, after 20 h. In addition, performing the reaction of complex **7** with the same concentration of aniline and temperature under a constant flow of argon (which could remove free ethylene) did

Scheme 8

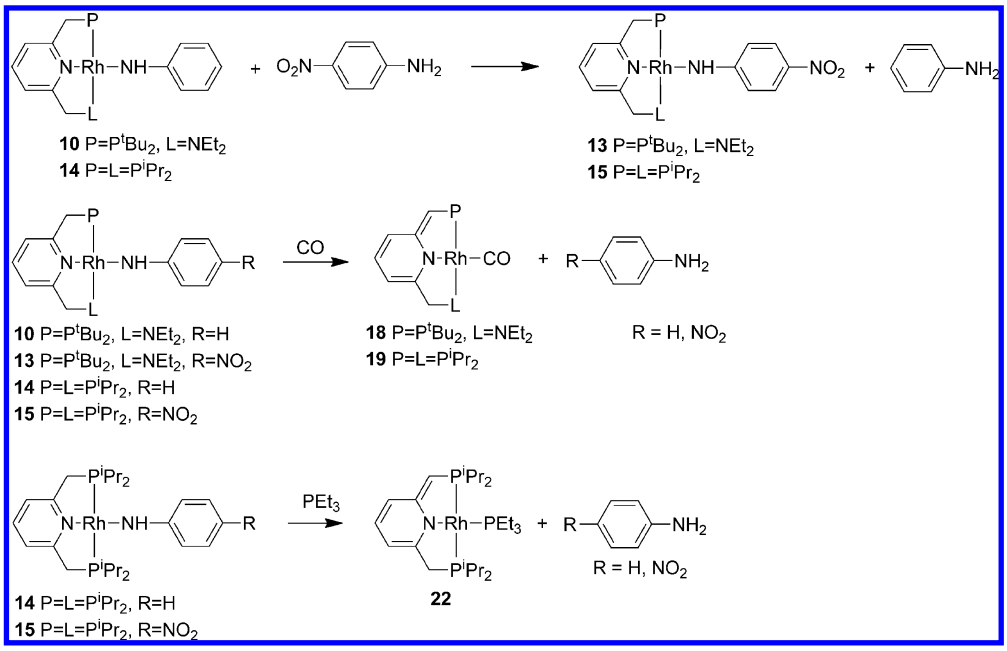

dx.doi.org/10.1021/om300248r | *Organometallics* 2012, 31, 4083−4101

Scheme 9

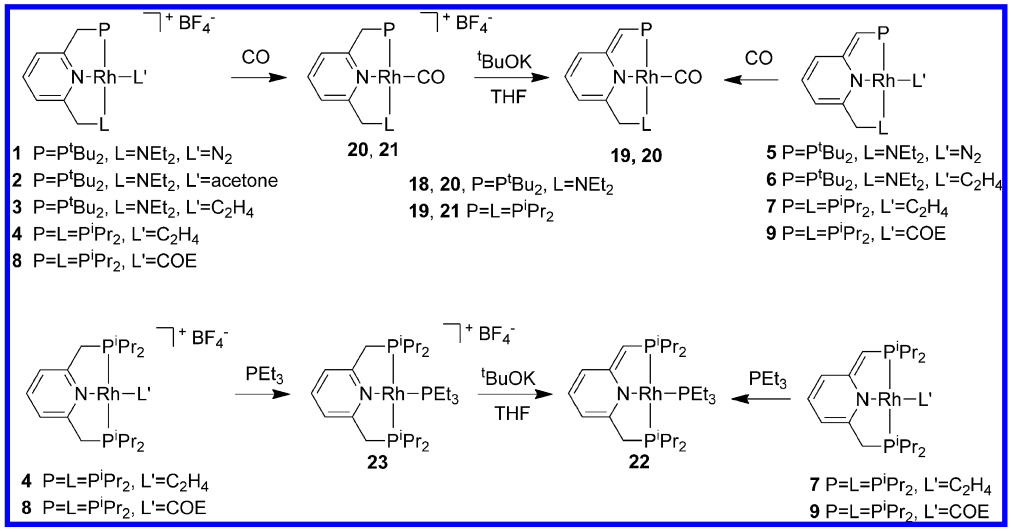

Scheme 10

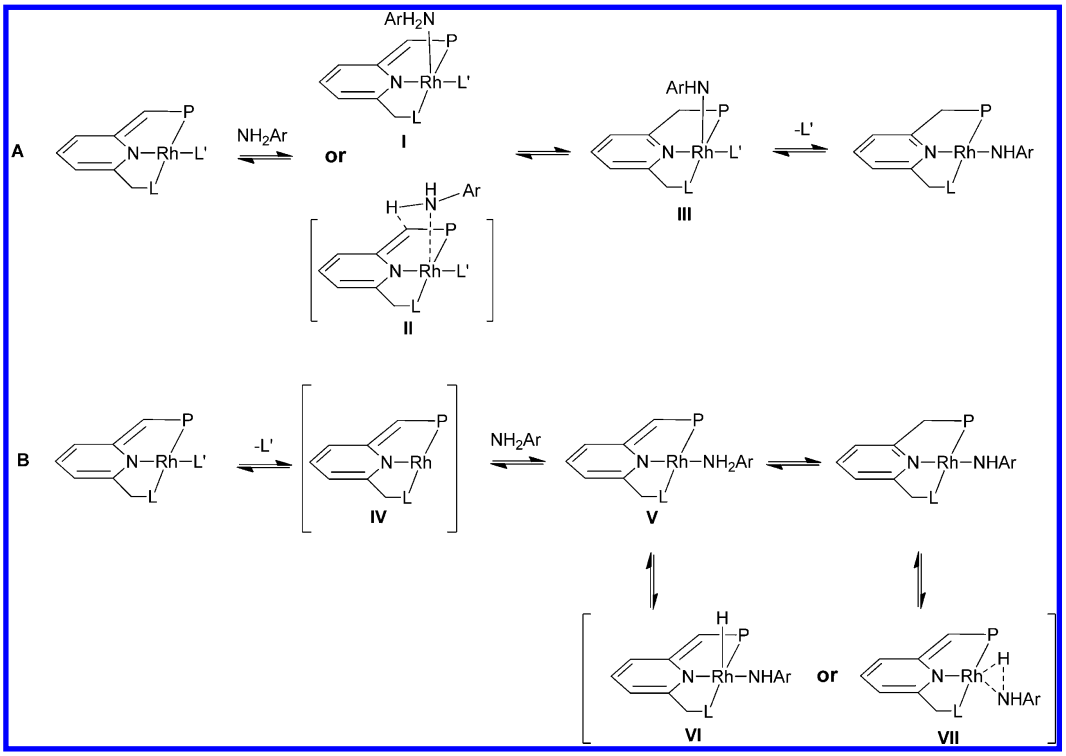

not influence the reaction rate. Performing the reactions of complexes **5**–**7** and **9** with 4 equiv of aniline did not influence the reaction rates.

Follow-up of the reaction of complexes **5** and **5a** by $^{31}P\{^{1}H\}$ NMR with anilines reveals that the mononuclear **5** reacts faster than the binuclear **5a** and it is the first to be fully consumed. The reaction rates were similar in toluene, benzene, or THF under the same conditions.

The reaction of complexes **5**–**7** and **9** with aniline and *p*-nitroaniline were followed by $^{31}P\{^{1}H\}$ and ^{1}H NMR spectroscopy also at low temperatures (in the range of 283–200 K); however, no intermediates were detected.

SST experiments were preformed with complexes **5**–**7** and **9** at 283 K in the presence of an excess of aniline. $^{31}P\{^{1}H\}$ NMR spectra of the reaction mixtures preformed prior to and after the SST experiments exhibit only signals of the starting complexes. Upon selective saturation of the deprotonated benzylic arms of complexes **5**–**7** and **9**, an SST effect was observed for the free aniline signal, indicating fast chemical exchange between the free aniline and the benzylic arm.

N–H Bond Formation; Elimination of Anilines. Fast elimination of anilines from complexes **10**–**15** was observed upon reaction with CO at ambient temperature. Along with the free anilines, which were detected both by ^{1}H NMR and by GC-MS, the deprotonated carbonyl complexes **18** and **19** were isolated (Scheme 8). Complexes **18** and **19** can be obtained also by addition of CO to the dearomatized complexes **5**–**7** and **9** or by deprotonation of the cationic carbonyl complexes [(PNN)Rh(CO)][BF_4] (**20**) and [(^{i}PrPNP)Rh(CO)][BF_4] (**21**) (Scheme 9). The $^{31}P\{^{1}H\}$ NMR spectrum of the reaction

dx.doi.org/10.1021/om300248r | *Organometallics* 2012, 31, 4083–4101

mixture of complex **15** and CO at 195 K exhibits signals of complexes **15** and **19** exclusively. An SST experiment performed with the deprotonated carbonyl complex **18** in the presence of an excess of aniline exhibits proton exchange between the deprotonated benzylic arm and the free aniline, although no aniline addition product was observed.

When complexes **10**, **13**, **14**, and **15** were exposed to a large excess of triethylphosphine at ambient temperature, no reaction took place.[58] However, upon heating the reaction mixtures of complexes **14** and **15** at 60 °C for 12 h, full conversion to form the dearomatized complex [(^{i}PrPNP*)Rh(PEt$_3$)] (**22**) along with the corresponding free anilines were observed (Scheme 8). Complex **22** can be synthesized independently by addition of the free phosphine to complexes **4** or **8**, followed by deprotonation or by addition of triethylphosphine to the dearomatized complex **7** or **9** (Scheme 9). Upon heating complexes **10** and **13** with an excess of triethylphosphine at 60 °C for 12 h, 90% of complex **10** and 33% of complex **13** reacted to give a mixture of unidentified complexes.[59]

The addition of 1 equiv of *p*-nitroaniline to the anilide complexes **10** and **14** affords the *p*-nitroanilide complexes **13** and **15**, respectively, and free aniline, which was detected by ^{1}H{^{31}P}NMR spectroscopy and GC-MS (Scheme 8).[60]

Possible Mechanisms of N–H Activation and Elimination. Possible mechanisms for the N–H bond activation process and its microscopic reverse N–H bond formation by the PNN– and ^{i}PrPNP–Rh(I) dearomatized complexes are described in Scheme 10. Pathway A represents an associative mechanism, in which preliminary coordination of the aniline derivative leads to proton transfer from the aniline to the deprotonated benzylic arm. The aniline can coordinate to the metal center at the apical position (complex **I**) or add in a concerted fashion (complex **II**), involving direct protonation of the benzylic arm by the aniline.[61] Mechanism A is similar to the postulated mechanism for N–H activation by [(^{t}BuPNP*)Ru(CO)H].[36] The activation of ND$_3$ by [(^{t}BuPNP*)Ru(CO)H] was highly stereospecific and occurred only on one face of the ligand, which supports an intramolecular mechanism with one coordinated molecule of ND$_3$. Since, in the case of complexes **5**–**7** and **9**, two empty apical positions are available for precoordination, such selectivity is not expected. It is worth mentioning that, upon follow-up of the reactions of complexes **5**–**7** and **9** with anilines at various temperatures (190–313 K) by ^{31}P{^{1}H} NMR spectroscopy, the potential intermediates **I**–**III** were not detected.

Pathway B is a dissociative mechanism, in which a tricoordinate dearomatized intermediate **IV** is formed and binds aniline to give the square-planar **V**. Intermediate **V** can activate the N–H bond either by oxidative addition (complex **VI**) or by a concerted mechanism (complex **VII**), followed by proton migration to the side arm with concomitant aromatization to form the aromatic anilide complex. Such a mechanism was observed for C–H activation by the complexes [(^{t}BuPNP*)RhCl][K][15] and [(^{t}BuPNP*)Ir(COE)].[13] In the case of the latter, DFT calculations suggest that one or two molecules of water may serve as a "proton shuttle" for the proton transfer from the metal center to the benzylic arm. The transition state of the proton transfer was found to be lower by 9.4 and 15.2 kcal mol^{-1} for one or two molecules of water involved, respectively, than the direct proton transfer.[14] In the case of pathway B, water may play a role in a proton transfer from the relatively remote aniline to the benzylic arm. As in the case of intermediates **I**–**III**, also intermediates **V**–**VII** were not detected.

The existence of an associative pathway A is supported by the following experimental evidence: (a) The N–H activation rate of *p*-nitroaniline was found to be faster with the ethylene complex **7**, in which ethylene is more tightly bound and less bulky than the COE complex **9**.[62] (b) N–H activation by complex **9** was significantly accelerated in the presence of COE.[63] (c) N–H activation of aniline by complex **7** was not accelerated when preformed in an open system. (d) The existence of fast exchange between the benzylic arm protons and the NH–anilide proton, as well as the proton exchange between free aniline and the benzylic arm prior to the N–H activation, as observed in the SST experiments also supports pathway A. (e) The fact that the N–H activation and elimination reactions are effected by steric factors is also in accordance with pathway A.

Deprotonation of the Anilide Complexes to Give Anionic Rh(I) Complexes. Recently, our group has reported several *anionic* dearomatized pincer complexes; the complex [(^{t}BuPNP*)RhCl][K], which was obtained by deprotonation of the complex [(^{t}BuPNP)RhCl] under argon,[15] the complex [(PNN*)Pt^{II}(Cl)(R)][Li] (R = CH$_3$, C$_6$H$_5$) with a decoordinated hemilabile amine arm,[64a] and the anionic doubly deprotonated complexes [(^{t}BuPNP**)M^{II}(X)]Y (^{t}BuPNP** = doubly deprotonated PNP; M = Pd, Pt; X = Cl, Me; Y = Li, K).[64b] These complexes constitute uncommon examples of anionic transition-metal complexes lacking strong π-acceptor ligands (capable of lowering the electron density at the metal center), such as CO, olefins, or electron-withdrawing phosphines.[64]

Here, we report on the anionic complexes [(PNN*)Rh(*p*-NO$_2$-NHC$_6$H$_4$)][K] (**24**) and [(^{i}PrPNP*)Rh(*p*-NO$_2$-NHC$_6$H$_4$)][K] (**25**), which were obtained by deprotonation of complexes **13** and **15**, respectively, by various bases (^{t}BuOK, KN(SiMe$_3$)$_3$, and KH) (Scheme 11). The electron-withdrawing

Scheme 11

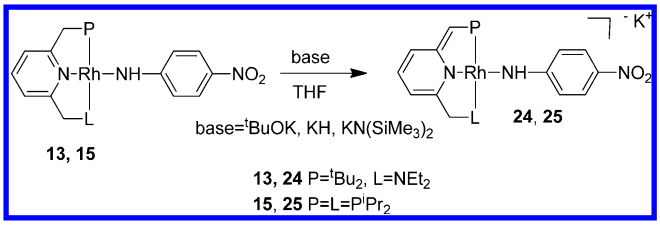

p-nitroanilide plays an important role in the stabilization of the anionic complexes, since the deprotonation of complexes **10** and **14** did not yield anionic complexes. Complexes **24** and **25** are stable in solution; however, under vacuum, partial decomposition took place, probably due to traces of water. Complexes **24** and **25** were fully characterized by NMR. The ^{31}P{^{1}H} NMR spectrum of **24** exhibits a sharp doublet at 80.09 ppm ($^{1}J_{RhP}$ = 206.9 Hz). The dearomatized phosphine arm of complex **24** gives rise to a one-proton signal at 3.10 ppm and a CH signal at 63.54 ppm in the ^{1}H and ^{13}C{^{1}H} NMR spectra, respectively. The amine benzylic arm of complex **24** gives rise to a two-proton signal at 3.46 ppm and a CH$_2$ signal at 64.89 ppm. Complex **25** exhibits a characteristic AB pattern of doublets at 46.07 (dd, $^{1}J_{RhP}$ = 150.5 Hz, $^{2}J_{PP}$ = 314.2 Hz) and 39.65 (dd, $^{1}J_{RhP}$ = 148.7 Hz, $^{2}J_{PP}$ = 314.2 Hz), indicating nonequivalent phosphorus atoms. The deprotonated benzylic

dx.doi.org/10.1021/om300248r | *Organometallics* 2012, 31, 4083–4101

arm gives rise to a one-proton signal at 3.24 ppm and a CH signal at 59.4 ppm, while the second benzylic arm gives rise to a two-proton signal at 2.90 ppm and a CH_2 signal at 36.15 ppm.

SUMMARY

It is evident that metal−ligand cooperation by pincer complexes, based on aromatization−dearomatization of the pincer ligand, can play an important role in bond activation and in the development of new homogeneously catalyzed reactions. Several X−H bonds (X = H, C, O, N) have been activated in this fashion. This study demonstrates a rare case of N−H activation by metal−ligand cooperation, as well as a rare example of N−H activation by Rh. The reverse reaction, N−H bond formation by metal−ligand cooperation, is also demonstrated. Thus, the new dearomatized complexes [(PNN*)RhL′] (**5**, L′ = N_2; **6**, L′ = C_2H_4) and [(^{i}PrPNP*)-RhL′] (**7**, L′ = C_2H_4; **9**, L′ = COE) react with anilines to give aromatized stable anilide complexes [(PNL)Rh(NHAr)] (PNL = PNN, ^{i}PrPNP; Ar = C_6H_5, *o*-Br-C_6H_4, *m*-Cl-*p*-Cl-C_6H_3, *p*-NO_2-C_6H_4). N−H formation to give free anilines and dearomatized Rh(I) complexes takes place upon reaction of the anilide complexes with CO or PEt_3. Spin saturation transfer experiments with the anilide complexes indicate proton exchange between the NH−anilide and the benzylic arm of the pincer ligand prior to and subsequent to the N−H activation; however, for *p*-nitroanilide complexes, such a chemical exchange was not observed. The N−H activation process is affected by electronic and steric factors. Anilines possessing electron-withdrawing groups accelerate the N−H activation and yield more stable anilide complexes, whereas bulky anilines and bulky pincer ligands retard the activation. Our studies suggest that the N−H activation and elimination occurs via an associative mechanism. In addition, deprotonation of complexes [(PNL)Rh(*p*-NO_2-$NH_2C_6H_4$)] (**13**, P = P^{t}Bu$_2$, L = NEt_2; **15**, P = L = P^{i}Pr$_2$) yields the dearomatized anionic complexes [(PNL*)Rh(*p*-NO_2-$NH_2C_6H_4$)].

Further experimental and theoretical investigations on metal−ligand cooperation via aromatization−dearomatization, and its implications for catalytic design, are in progress. While the reported cases so far involve bonds to hydrogen, and mostly late transition-metal complexes, we believe that the scope of this approach can be even wider.

EXPERIMENTAL SECTION

General Procedures. All experiments with metal complexes and phosphine ligands were carried out under an atmosphere of purified nitrogen in a Vacuum Atmospheres glovebox equipped with a MO 40-2 inert gas purifier or using standard Schlenk techniques. All solvents were reagent grade or better. All nondeuterated solvents, except methylene chloride and acetone, were refluxed over sodium/benzophenone ketyl and distilled under an argon atmosphere. Methylene chloride and acetone were used as received and dried over 4 Å molecular sieves and calcium sulfate, respectively. Deuterated solvents were used as received. All the solvents were degassed with argon and kept in the glovebox over 4 Å molecular sieves (acetone was kept over calcium sulfate). Other commercially available reagents were used as received.

The ^{i}PrPNP[65] and PNN[2a] ligands, $[Rh(COE)_2Cl]_2$,[66] $[Rh(C_2H_4)_2(Cl\text{-}\mu)]_2$,[67] and [(^{i}PrPNP)Rh(COE)][BF_4][49] (**8**) were prepared according to literature procedures. The previously reported complex [(^{t}BuPNP)Rh(N_2)][BF_4][15,51] was prepared by the procedure described below for the synthesis of complex **1**. ^{1}H, ^{13}C, and ^{31}P NMR spectra were recorded using Bruker DPX-250, Bruker Avance-400 NMR, and Bruker Avance 500 NMR spectrometers. All spectra were recorded at 23 °C unless otherwise noted. ^{1}H NMR and $^{13}C\{^1H\}$ NMR chemical shifts are reported in parts per million (ppm) downfield from tetramethylsilane. In ^{1}H NMR, the chemical shifts were referenced to the residual hydrogen signal of the deuterated solvents. In $^{13}C\{^1H\}$ NMR measurements, the signals of deuterated solvents were used as a reference. ^{31}P NMR chemical shifts are reported in parts per million downfield from H_3PO_4 and referenced to an external 85% solution of phosphoric acid in D_2O. Abbreviations used in the description of NMR data are as follows: br, broad; s, singlet; d, doublet; t, triplet; q, quartet; m, multiplet; v, virtual. Temperature calibration of the spectrometer was performed using CH_3OH/CD_3OD. IR spectra were measured with a Nicolet-6700 FT-IR spectrometer. Elemental analyses were performed by the Unit of Chemical Research Support, Weizmann Institute of Science.

[(PNN)RhN$_2$][BF$_4$] (1). $[Rh(COE)_2Cl]_2$ (118.0 mg, 0.165 mmol) and $AgBF_4$ (64.2 mg, 0.330 mmol) were suspended in THF (5 mL) under nitrogen, and the suspension was stirred in the dark for 1 h, resulting in precipitation of a light gray solid (AgCl), which was filtered off through a 0.2 μm Teflon filter. A THF solution (3 mL) of the PNN ligand (106.4 mg, 0.330 mmol) was immediately added to the filtrate. The reaction was stirred for 24 h, during which a yellow precipitate was formed. The precipitate was collected by vacuum filtration, washed with THF (7 mL), and dried under vacuum. Yield: 102.6 mg (57%). Crystals suitable for X-ray analysis of **1a** were obtained by layering a concentrated acetone solution of **1a** with pentane.

$^{31}P\{^1H\}$ NMR (121 MHz, acetone-d_6, 293 K): 93.31 (d, $^1J_{RhP}$ = 161.6 Hz). ^{1}H NMR (500 MHz, acetone-d_6, 293 K): 1.47 (d, 18H, $^3J_{HP}$ = 14.0 Hz, $(CH_3)_3CP$), 1.52−1.79 (br m, 6H, CH_3CH_2N), 3.14−3.26 (m, 2H, CH_3CH_2N), 3.27−3.37 (m, 2H, CH_3CH_2N), 3.77 (d, 2H, $^2J_{HP}$ = 9.5 Hz, CH_2P), 4.55 (br m, 2H, Py-CH_2N), 7.45 (d, 1H, $^3J_{HH}$ = 7.8 Hz, Py-CH), 7.56 (d, 1H, $^3J_{HH}$ = 7.8 Hz, Py-CH), 7.95 (t, 1H, $^3J_{HH}$ = 7.8 Hz, Py-CH). ^{1}H NMR (500 MHz, acetone-d_6, 253 K): 1.45 (d, 9H, $^3J_{HP}$ = 14.0 Hz, $(CH_3)_3CP$), 1.46 (d, 9H, $^3J_{HP}$ = 14.0 Hz, $(CH_3)_3CP$), 1.52 (t, 3H, $^3J_{HH}$ = 7.0 Hz, CH_3CH_2N), 1.72 (t, 3H, $^3J_{HH}$ = 7.0 Hz, CH_3CH_2N), 3.11−3.24 (m, 2H, CH_3CH_2N), 3.24−3.37 (m, 2H, CH_3CH_2N), 3.80 (d, 2H, $^2J_{HP}$ = 9.4 Hz, CH_2P), AB system centered at 4.49 (d, $^2J_{HH}$ = 17.0 Hz, Py-CH_2N) and 4.75 (d, $^2J_{HH}$ = 17.0 Hz, Py-CH_2N), 7.45 (d, 1H, $^3J_{HH}$ = 7.8 Hz, Py-CH), 7.56 (d, 1H, $^3J_{HH}$ = 7.8 Hz, Py-CH), 7.95 (t, 1H, $^3J_{HH}$ = 7.8 Hz, Py-CH). $^{13}C\{^1H\}$ NMR (75 MHz, acetone-d_6, 293 K): 12.60 (s, CH_3CH_2N), 29.46 (d, $^2J_{CP}$ = 4.5 Hz, $(CH_3)_3CP$), 35.02 (d, $^1J_{CP}$ = 24.1 Hz, CH_2P), 35.76 (br d, $^1J_{CP}$ = 16 Hz, $(CH_3)_3CP$), 56.3 (br m, CH_3CH_2N), 63.49 (d, J = 2.0 Hz, Py-CH_2N), 119.77 (s, Py-CH), 120.20 (d, $^3J_{CP}$ = 10.6 Hz, Py-CH), 139.34 (s, Py-CH), 164.12−164.28 (m, Py-C2 and Py-C5). IR(ν_{NN}) = 2069, 2157 cm^{-1}. Anal. for $C_{38}H_{70}B_2F_8N_6P_2Rh_2$: Calcd C, 43.37; H, 6.70. Found: C, 43.37; H, 6.75.

X-ray structural analysis of **1a**. Crystal data: $C_{38}H_{70}N_6P_2Rh_2$ + C_3H_6O + $2BF_4$, orange chunk, 0.20 × 0.10 × 0.10 mm^3, monoclinic, $P2_1/c$, a = 18.5320(4) Å, b = 15.3840(4) Å, c = 18.8970(4) Å, β = 109.264 (1)°, from 10 687 reflections, T = 120(2) K, V = 5085.8(2) Å^3, Z = 4, F_w = 1110.46, D_c = 1.450 Mg/m^{-3}, μ = 0.778 mm^{-1}.

Data collection and processing: Nonius KappaCCD diffractometer, Mo Kα (λ = 0.71073 Å), graphite monochromator, $-24 \le h \le 21$, $-19 \le k \le 19$, $-22 \le l \le 24$, $2\theta_{max}$ = 55.06, frame scan width = 1.0°, scan speed = 1.0° per 150 s, typical peak mosaicity 1.421°, 56 613 reflections collected, 11 652 independent reflections (R_{int} = 0.068). The data were processed with HKL2000.

Solution and refinement: Structure solved by direct methods with SIR-97. Full-matrix least-squares refinement based on F^2 with SHELXL-97. 565 parameters with no restraints, final R_1 = 0.0392 (based on F^2) for data with $I > 2\sigma(I)$, R_1 = 0.0740 on 11 652 reflections, goodness-of-fit on F^2 = 1.081, largest electron density peak = 1.090 e Å^{-3}, and largest hole = −0.719 e Å^{-3}.

[(PNN)Rh(acetone)][BF$_4$] (2). $[Rh(COE)_2Cl]_2$ (72.4 mg, 0.101 mmol) and $AgBF_4$ (39.3 mg, 0.202 mmol) were suspended in acetone (5 mL) under argon, and the suspension was stirred in the dark for 1 h, resulting in the precipitation of a light gray solid (AgCl). The precipitate was filtered off through a 0.2 μm Teflon filter. An acetone solution (3 mL) of the PNN ligand (65.2 mg, 0.202 mmol) was

dx.doi.org/10.1021/om300248r | Organometallics 2012, 31, 4083−4101

immediately added to the filtrate, and the reaction mixture was stirred for 10 min. The solvent was removed under vacuum to give an orange oil, which was washed with pentane (15 mL) and dried under vacuum. Yield: 84% (96.8 mg). Crystals suitable for X-ray analysis were obtained by layering a concentrated acetone solution of **2** with pentane.

$^{31}P\{^{1}H\}$ NMR (121 MHz, acetone-d_6): 86.85 (d, $^{1}J_{RhP}$ = 193.4 Hz). ^{1}H NMR (500 MHz, acetone-d_6): 1.36 (d, 18H, $^{3}J_{HP}$ = 13.1 Hz, $(CH_3)_3CP$), 1.46 (t, 6H, $^{3}J_{HH}$ = 7.2 Hz, CH_3CH_2N), 2.86−2.77 (m, 2H, CH_3CH_2N), 2.91−3.00 (m, 2H, CH_3CH_2N), 3.19 (d, 2H, $^{2}J_{HP}$ = 8.9 Hz, CH_2P), 4.20 (br s, 2H, Py-CH_2N), 7.17 (d, 1H, $^{3}J_{HH}$ = 7.9 Hz, Py-CH), 7.26 (d, 1H, $^{3}J_{HH}$ = 7.9 Hz, Py-CH), 7.70 (t, 1H, $^{3}J_{HH}$ = 7.9 Hz, Py-CH). $^{13}C\{^{1}H\}$ NMR (101 MHz, acetone-d_6): 10.81 (s, CH_3CH_2N), 29.24 (d, $^{2}J_{CP}$ = 5.6 Hz, $(CH_3)_3CP$), 35.02 (dd, $^{1}J_{CP}$ = 16.1 Hz, $^{2}J_{CRh}$ = 1.5 Hz, $(CH_3)_3CP$), 35.56 (dd, $^{1}J_{CP}$ = 22.1 Hz, $^{2}J_{CRh}$ = 2.1 Hz, CH_2P), 52.47 (d, J = 1.6 Hz, CH_3CH_2N), 64.42 (d, J = 2.2 Hz, Py-CH_2N), 119.80 (s, Py-CH), 121.71 (dd, $^{3}J_{CP}$ = 11.0 Hz, $^{3}J_{CRh}$ = 1.5 Hz, Py-CH), 133.72 (s, Py-CH), 161.60 (br d, J = 1.6 Hz, Py-C), 163.67 (dd, $^{2}J_{CP}$ = 22.1 Hz, $^{2}J_{CRh}$ = 2.1 Hz, Py-C), 223.28 (s, $(CH_3)_2CO$). Acceptable elemental analysis results for **2** could not be obtained. The NMR spectrum of **2** appears in the Supporting Information.

X-ray structural analysis of **2**. Crystal data: $C_{22}H_{41}N_2OPRh + BF_4$, orange plates, 0.20 × 0.10 × 0.10 mm^3, monoclinic, $P2_1/c$, a = 11.1560(1) Å, b = 14.3340(2) Å, c = 16.5290(3) Å, β = 90.1630(6)°, from 11 771 reflections, T = 120(2) K, V = 2643.14(6) Å^3, Z = 4, F_w = 570.26, D_c = 1.433 Mg/m^{-3}, μ = 0.751 mm^{-1}.

Data collection and processing: Nonius KappaCCD diffractometer, Mo Kα (λ = 0.71073 Å), graphite monochromator, $-16 \le h \le 16$, $-16 \le k \le 21$, $-24 \le l \le 23$, $2\theta_{max}$ = 64.06, frame scan width = 1.0°, scan speed = 1.0° per 20 s, typical peak mosaicity 0.467°, 40 760 reflections collected, 16 760 independent reflections (R_{int} = 0.053). The data were processed with HKL2000 software.

Solution and refinement: Structure solved by direct methods with SIR-97. Full-matrix least-squares refinement based on F^2 with SHELXL-97. 299 parameters with no restraints, final R_1 = 0.0322 (based on F^2) for data with $I > 2\sigma(I)$, R_1 = 0.0432 on 8992 reflections, goodness-of-fit on F^2 = 1.030, largest electron density peak = 1.215 e Å^{-3}, and largest hole = −0.645 e Å^{-3}.

[(PNN)Rh(C_2H_4)][BF_4] (3). $[Rh(C_2H_4)_2Cl]_2$ (60.0 mg, 0.154 mmol) and $AgBF_4$ (60.0 mg, 0.308 mmol) were suspended in acetone (5 mL) under nitrogen, and the reaction was stirred in the dark for 1 h, resulting in the precipitation of a light gray solid (AgCl). The precipitate was filtered off through a 0.2 μm Teflon filter. An acetone solution (3 mL) of the PNN ligand (99.3 mg, 0.308 mmol) was immediately added to the filtrate, and the reaction mixture was stirred for 10 min. The solvent was removed under vacuum, and the yellow solid was washed with pentane (15 mL) and dried under vacuum. Yield: 95% (158.1 mg)

Crystals suitable for X-ray analysis were obtained by layering a concentrated acetone solution of **3** with pentane.

$^{31}P\{^{1}H\}$ NMR (121 MHz, acetone-d_6): 81.65 (d, $^{1}J_{RhP}$ = 168.9 Hz). ^{1}H NMR (500 MHz, acetone-d_6): 1.35 (d, 18H, $^{3}J_{HP}$ = 13.3 Hz, $(CH_3)_3CP$), 1.40 (t, 6H, $^{3}J_{HH}$ = 7.1 Hz, CH_3CH_2N), 2.69−2.78 (m, 2H, CH_3CH_2N), 2.92−2.99 (m, 2H, CH_3CH_2N), 3.52 (br s, 4H, $CH_2{=}CH_2$), 3.77 (d, 2H, $^{2}J_{HP}$ = 9.3 Hz, CH_2P), 4.39 (s, 2H, Py-CH_2N), 7.57 (d, 1H, $^{3}J_{HH}$ = 7.7 Hz, Py-H), 7.74 (d, 1H, $^{3}J_{HH}$ = 7.8 Hz, Py-H), 8.07 (t, 1H, $^{3}J_{HH}$ = 7.8 Hz, Py-H). $^{13}C\{^{1}H\}$ NMR (125 MHz, acetone-d_6): 12.61 (s, CH_3CH_2N), 29.75 (d, $^{2}J_{CP}$ = 3.8 Hz, $(CH_3)_3CP$), 36.85 (dd, $^{1}J_{CP}$ = 13.6 Hz, $^{2}J_{CRh}$ = 1.8 Hz, $(CH_3)_3CP$, overlapping with the doublet signal at 37.08 ppm), 37.08 (d, $^{2}J_{CP}$ = 23.8 Hz, CH_2P, overlapping with the doublet of doublet signal at 36.85 ppm), 54.00 (br s, CH_3CH_2N), 59.72 (d, $^{1}J_{RhP}$ = 12.7 Hz, $CH_2{=}CH_2$), 65.15 (d, J = 1.8 Hz, Py-CH_2N), 119.66 (s, Py-CH), 122.04 (d, $^{3}J_{CP}$ = 10.2 Hz, Py-CH), 141.39 (s, Py-CH), 163.48 (br s, Py-C), 163.56 (m, Py-C). Anal. for $C_{21}H_{39}BF_4N_2PRh$: Calcd C, 46.69; H, 7.28. Found: C, 46.80; H, 7.27.

X-ray structural analysis of **3**. Crystal data: $C_{21}H_{39}N_2PRh + BF_4$, orange prisms, 0.25 × 0.22 × 0.18 mm^3, triclinic, $P\bar{1}$, a = 7.8170(1) Å, b = 11.8504(2) Å, c = 13.9795(2) Å, α = 74.3341(10)°, β = 74.2262(10)°, γ = 85.5839(6)° from 10° of data, T = 120(2) K, V = 1199.92(3) Å^3, Z = 2, F_w = 540.23, D_c = 1.495 Mg/m^{-3}, μ = 0.820 mm^{-1}.

Data collection and processing: Nonius KappaCCD diffractometer, Mo Kα (λ = 0.71073 Å), graphite monochromator, $0 \le h \le 10$, $-15 \le k \le 15$, $-16 \le l \le 18$, $2\theta_{max}$ = 54.96, frame scan width = 1.0°, scan speed = 1.0° per 30 s, typical peak mosaicity 0.69°, 23 846 reflections collected, 5500 independent reflections (R_{int} = 0.027). The data were processed with HKL-scalepack software.

Solution and refinement: Structure solved by direct methods with SHELXS. Full-matrix least-squares refinement based on F^2 with SHELXL-97. 295 parameters with no restraints, final R_1 = 0.0305 (based on F^2) for data with $I > 2\sigma(I)$, R_1 = 0.0334 on 5500 reflections, goodness-of-fit on F^2 = 1.099, largest electron density peak = 1.390 e Å^{-3}, and largest hole = −0.868 e Å^{-3}.

[(^{i}PrPNP)Rh(C_2H_4)][BF_4] (4). $[Rh(C_2H_4)_2Cl]_2$ (42.0 mg, 0.108 mmol) and $AgBF_4$ (42.0 mg, 0.216 mmol) were suspended in acetone (5 mL) under nitrogen, and the suspension was stirred in the dark for 1 h, resulting in the precipitation of a light gray solid (AgCl). The precipitate was filtered off through a 0.2 μm Teflon filter. An acetone solution (3 mL) of ^{i}PrPNP (73.2 mg, 0.216 mmol) was immediately added to the filtrate, and the reaction mixture was stirred for 10 min to give a clear brown solution. The solvent was removed under vacuum, and the brown solid was washed with pentane (15 mL) and dried under vacuum. Yield: 96% (115.4 mg). Crystals suitable for X-ray analysis were obtained by layering a concentrated acetone solution of **4** with pentane.

$^{31}P\{^{1}H\}$ NMR (121 MHz, acetone-d_6): 53.90 (d, $^{1}J_{RhP}$ = 122.4 Hz). ^{1}H NMR (500 MHz, acetone-d_6): 1.17 (dd, 12 H, $^{3}J_{PH}$ = 7.0 Hz, $^{3}J_{HH}$ = 7.3 Hz, $(CH_3)_2CH$), 1.26 (dd, 12H, $^{3}J_{PH}$ = 8.7 Hz, $^{3}J_{HH}$ = 7.3 Hz, $(CH_3)_2CH$), 2.40−2.51 (m, 4H, $(CH_3)_2CH$), 3.51 (dt, 4H, $^{3}J_{PH}$ = 3.3 Hz, $^{2}J_{RhH}$ = 2.2 Hz (coupling constant were detriment also by $^{1}H\{^{31}P\}$ NMR), $CH_2{=}CH_2$), 3.80 (vt, 4H, J_{PH} = 4.1 Hz, CH_2P), 7.69 (d, 1H, $^{3}J_{HH}$ = 7.7 Hz, Py-CH), 8.00 (t, 2H, $^{3}J_{HH}$ = 7.7 Hz, Py-CH). $^{13}C\{^{1}H\}$ NMR (126 MHz, acetone-d_6): 19.02 (s, $(CH_3)_2CH$), 19.80 (vt, J_{PC} = 2.3 Hz, $(CH_3)_2CH$), 25.82 (d vt, $^{2}J_{RhC}$ = 1.5 Hz, J_{PC} = 11.7 Hz, $(CH_3)_2CH$), 36.98 (vt, J_{PC} = 9.8 Hz, CH_2P), 52.34 (dt, $^{1}J_{RhC}$ = 10.7 Hz, $^{2}J_{PC}$ = 1.7 Hz, $CH_2{=}CH_2$), 122.36 (d vt, $^{3}J_{RhC}$ = 0.7 Hz, J_{PC} = 5.4 Hz, Py-CH), 141.62 (s, Py-CH), 166.51 (d vt, $^{2}J_{RhC}$ = 1.6 Hz, J_{PC} = 5.3 Hz, Py-C). Anal. for $C_{21}H_{39}BF_4NP_2Rh$: Calcd C, 45.27; H, 7.05. Found: C, 45.92; H, 7.23.

X-ray structural analysis of **4**. Crystal data: $C_{21}H_{39}NP_2Rh + BF_4$, orange needles, 0.50 × 0.05 × 0.05 mm^3, monoclinic, $P2_1/n$, a = 11.6467(5) Å, b = 16.1779(8) Å, c = 13.9470(8) Å, β = 104.855(3)°, from 21 485 reflections, T = 120(2) K, V = 2540.1(2) Å^3, Z = 4, F_w = 557.19, D_c = 1.457 Mg/m^{-3}, μ = 0.836 mm^{-1}.

Data collection and processing: Bruker KappaApexII CCD diffractometer, Mo Kα (λ = 0.71073 Å), graphite monochromator, $-16 \le h \le 17$, $-24 \le k \le 15$, $-18 \le l \le 20$, $2\theta_{max}$ = 66.44, frame scan width = 0.5°, scan speed = 1.0° per 40 s, typical peak mosaicity 0.71°, 21 113 reflections collected, 9862 independent reflections (R_{int} = 0.0504). The data were processed with APEX2.

Solution and refinement: Structure solved by direct methods with Bruker AutoStructure. Full-matrix least-squares refinement based on F^2 with SHELXL-97. 283 parameters with no restraints, final R_1 = 0.0468 (based on F^2) for data with $I > 2\sigma(I)$, R_1 = 0.0843 on 9570 reflections, goodness-of-fit on F^2 = 0.958, largest electron density peak = 1.457 e Å^{-3}, and largest hole = −1.211 e Å^{-3}.

[(PNN*)RhN_2] (5) and [((PNN*)Rh)$_2$)(N_2-μ)] (5a). To a suspension of [(PNN)RhN_2][BF_4] (**1**) (54.1 mg, 0.10 mmol) in THF (5 mL) under nitrogen was added a THF (5 mL) solution of ^{t}BuOK (12.3 mg, 0.11 mmol), and the reaction mixture turned red. The solution was stirred vigorously at ambient temperature overnight (or until the entire yellow solid (starting complex) disappeared), and the solvent was removed under vacuum. The residue was extracted with benzene, and the extracts were combined and filtered through a 0.2 μm Teflon filter. The solvent was removed under vacuum to give a mixture of complexes **5** and **5a** as a red solid (75.5 mg) in 78% yield. The assignment of the signals of complexes **5** and **5a** was done based on the mixture.

dx.doi.org/10.1021/om300248r | Organometallics 2012, 31, 4083−4101

$^{31}P\{^{1}H\}$ NMR (121 MHz, toluene-d_6, 293 K): 84.76 (d, 1P, $^{1}J_{RhP}$ = 173.7 Hz) (complex **5**, 75% by integration) and 83.51 (d, 2P, $^{1}J_{RhP}$ = 170.1 Hz) (complex **5a**, 25% by integration). ^{1}H NMR (300 MHz, toluene-d_6): 1.22 (t, $^{3}J_{HH}$ = 7.2 Hz, CH_3CH_2N **5a**), 1.34 (t, $^{3}J_{HH}$ = 7.2 Hz, CH_3CH_2N **5**), 1.47 (d, $^{3}J_{HP}$ = 13.0 Hz, $(CH_3)_3CP$ **5a**), 1.49 (d, $^{3}J_{HP}$ = 12.8 Hz, $(CH_3)_3CP$ **5**), 2.32−2.46 (m, CH_3CH_2N **5a**), 2.62−2.78 (m, CH_3CH_2N **5**), 2.78−2.95 (m, CH_3CH_2N **5**), 3.01 (br s, Py-CH_2N **5a**), 3.14 (br s, Py-CH_2N **5**), 3.38 (q, $^{1}J_{HP}$ = $^{2}J_{HRh}$ = 1.6 Hz, in $^{1}H\{^{31}P\}$ appears as a d, $^{1}J_{HP}$ = 1.6 Hz, CHP **5a**), 3.42 (dd, $^{1}J_{HP}$ = 1.5 Hz, $^{2}J_{HRh}$ = 1.1 Hz, in $^{1}H\{^{31}P\}$ appears as a d, $^{1}J_{HP}$ = 1.5 Hz, CHP **5**), 5.13−5.19 (m, Py-CH **5** + **5a**), 6.11 (br d, $^{3}J_{HH}$ = 8.7 Hz, Py-CH **5** + **5a**), 6.34−6.42 (m, Py-CH **5** + **5a**). $^{13}C\{^{1}H\}$ NMR (100 MHz, toluene-d_8): 11.94 (s, CH_3CH_2N **5** + **5a**), 29.83 (d, $^{2}J_{CP}$ = 5.2 Hz, $(CH_3)_3CP$ **5a**), 30.29 (d, $^{2}J_{CP}$ = 5.5 Hz, $(CH_3)_3CP$ **5**), 36.07 (d, $^{1}J_{CP}$ = 22.0 Hz, $(CH_3)_3CP$ **5**), 36.43 (br d, $^{1}J_{CP}$ = 24.4 Hz, $(CH_3)_3CP$ **5a**, 53.09 (d, J = 1.7 Hz, CH_3CH_2N **5a**), 54.42 (br s, CH_3CH_2N **5**), 62.70 (dd, $^{2}J_{RhC}$ = 1.1 Hz, $^{1}J_{PC}$ = 57.1 Hz, CH-P **5** or **5a**), 63.04 (d, J = 1.8 Hz, Py-CH_2N **5** or **5a** overlapping with another CH-P signal that could not be identified both in DEPT and in $^{13}C\{^{1}H\}$ NMR), 63.47 (d, J = 1.8 Hz, Py-CH_2N **5** or **5a**), 95.17 (s, Py-CH **5**), 96.02 (s, P-CH **5a**), 112.25 (d, $^{3}J_{CP}$ = 18.3 Hz, Py-CH **5**), 112.84 (d, $^{3}J_{CP}$ = 19.2 Hz, Py-CH **5a**), 131.14 (s, Py-CH **5**), 131.45 (s, Py-CH **5a**), 157.63 (d, J_{CP} = 1.4 Hz, Py-C **5a**), 158.78 (d, J_{CP} = 1.3 Hz, Py-C **5**), 169.90−170.19 (m, Py-C **5** + **5a**). IR(ν_{NN}) = 2110 cm^{-1}. Anal. for $C_{19}H_{34}N_2PRh$: Calcd C, 50.45; H, 7.58. Found: C, 50.50; H, 8.07.

[(PNN*)Rh(C_2H_4)] (6). Complex **6** was synthesized in the same manner as complex **5** from [(PNN)Rh(C_2H_4)][BF_4] (**3**) (64.9 mg, 0.120 mmol) and ^{t}BuOK (13.4 mg, 0.120 mmol), and the reaction mixture was stirred at ambient temperature for 30 min. Complex **6** was obtained as a red solid in 92% (50.0 mg) yield.

$^{31}P\{^{1}H\}$ NMR (121 MHz, benzene-d_6): 70.71 (d, $^{1}J_{RhP}$ = 177.4 Hz). ^{1}H NMR (300 MHz, benzene-d_6): 1.01 (t, 6H, $^{3}J_{HH}$ = 7.1 Hz, CH_3CH_2N), 1.38 (d, 18H, $^{3}J_{PH}$ = 12.3 Hz, $(CH_3)_3CP$), 1.86−1.94 (m, 2H, CH_3CH_2N), 2.08−2.20 (m, 2H, CH_3CH_2N), 2.86 (s, overlapping with the signal at 2.89, total integration 6H, assignment according to HSQC, CH_2═CH_2), 2.89 (s, overlapping with the signal at 2.86, total integration 6H, assignment according to HSQC, Py-CH_2N), 3.42 (br s, 1H, CH-P), 6.35 (d, 1H, $^{3}J_{HH}$ = 8.7 Hz, Py-H), 6.44−6.48 (m, 2H, Py-H). $^{13}C\{^{1}H\}$ NMR (101 MHz, benzene-d_6): 11.65 (s, CH_3CH_2N), 30.02 (d, $^{2}J_{CP}$ = 4.4 Hz, $(CH_3)_3CP$), 36.14 (dd, $^{1}J_{CP}$ = 20.4 Hz, $^{2}J_{CRh}$ = 1.9 Hz, $(CH_3)_3CP$), 48.86 (dd, $^{1}J_{CRh}$ = 13.2 Hz, $^{2}J_{CP}$ = 1.7 Hz, CH_2═CH_2), 52.19 (br s, CH_3CH_2N), 64.07 (d, J = 1.5 Hz, Py-CH_2N), 67.39 (d, $^{1}J_{CP}$ = 55.2 Hz, CH-P), 93.52 (s, Py-CH), 113.60 (d, $^{3}J_{CP}$ = 18.0 Hz, Py-CH), 132.28 (s, Py-CH), 158.23 (s, Py-C), 168.33−168.67 (m, Py-C). Acceptable elemental analysis results for **6** could not be obtained. The NMR spectrum of **6** appears in the Supporting Information.

[(^{i}PrPNP*)Rh(C_2H_4)] (7). Complex **7** was synthesized in the same manner as complex **5** from [(^{i}PrPNP)Rh(C_2H_4)][BF_4] (**4**) (81.3 mg, 0.146 mmol) and ^{t}BuOK (16.3 mg, 0.146 mmol), and the reaction mixture was stirred at ambient temperature for 30 min. Complex **7** was obtained as a red solid in 86% (59.0 mg) yield.

$^{31}P\{^{1}H\}$ NMR (121 MHz, benzene-d_6): AB system centered at 45.15 and 40.38 (dd, $^{1}J_{RhP}$ = 127.2 Hz, $^{2}J_{PP}$ = 322.5 Hz). ^{1}H NMR (500 MHz, benzene-d_6): 0.77−0.81 (m, 12H, $(CH_3)_2CH$), 0.86−0.91 (m, 6H, $(CH_3)_2CH$), 1.15−1.23 (m, 6H, $(CH_3)_2CH$), 1.44−1.52 (m, 2H, $(CH_3)_2CH$), 1.83−1.91 (m, 2H, $(CH_3)_2CH$), 2.44 (d, 2H, $^{2}J_{PH}$ = 9.2 Hz, CH_2-P), 3.20 (dt, 4H, $^{3}J_{PH}$ = 3.7 Hz, $^{2}J_{RhH}$ = 1.9 Hz (coupling constants were detriment also by $^{1}H\{^{31}P\}$ NMR), CH_2═CH_2), 3.35 (d, 1H, $^{2}J_{PH}$ = 4.0 Hz, CHP), 5.38 (br d, 1H, J = 5.5 Hz, Py-CH), 6.46−6.50 (m, 2H, Py-CH). $^{13}C\{^{1}H\}$ NMR (126 MHz, benzene-d_6): 17.77 (br d, $^{2}J_{PC}$ = 11 Hz, $(CH_3)_2CH$), 18.59 (d, $^{2}J_{PC}$ = 5.2 Hz, $(CH_3)_2CH$), 18.74 (d, $^{2}J_{PC}$ = 5.4 Hz, $(CH_3)_2CH$), 23.73 (ddd, J = 1.5, 3.4, 16.0 Hz, $(CH_3)_2CH$), 24.90 (ddd, J = 1.5, 3.5, 23.7 Hz, $(CH_3)_2CH$), 34.91 (d, $^{1}J_{PC}$ = 18.7 Hz, CH_2P), 44.51 (dt, $^{1}J_{RhC}$ = 11.7 Hz, $^{2}J_{PC}$ = 1.7 Hz, CH_2═CH_2), 63.36 (d, $^{1}J_{PC}$ = 50.8 Hz, CHP), 96.75 (dd, J = 0.5, 11.4 Hz, Py-CH), 114.75 (d, J_{PC} = 18.4 Hz, Py-CH), 132.12 (br s, Py-CH), 173.87 (dd, J = 2.4, 3.5 Hz, Py-C), 174.03 (dd, J = 2.5, 3.8 Hz, Py-C). Anal. for $C_{21}H_{38}NP_2Rh$: Calcd C, 53.74; H, 8.16. Found: C, 53.68; H, 8.27.

[(^{i}PrPNP*)Rh(COE)] (9). Complex **9** was synthesized in the same manner as complex **5** from [(^{i}PrPNP)Rh(COE)][BF_4] (**8**) (74.9 mg, 0.117 mmol) and ^{t}BuOK (13.1 mg, 0.117 mmol), and the reaction mixture was stirred at ambient temperature for 30 min. Complex **9** was obtained as a red solid in 96% (61.9 mg) yield. The NMR characterization of complex **9** was performed at 223 K since, at ambient temperature, only very broad signals were observed.

$^{31}P\{^{1}H\}$ NMR (202 MHz, toluene-d_8, 223 K): AB system centered at 32.63 (dd, $^{1}J_{RhP}$ = 136.2 Hz, $^{2}J_{PP}$ = 312.8 Hz) and 45.55 (dd, $^{1}J_{RhP}$ = 130.4 Hz, $^{2}J_{PP}$ = 312.8 Hz). ^{1}H NMR (500 MHz, toluene-d_8, 223 K): 0.74 (dd, 6H, J = 7.3, 10.9 Hz, $CH(CH_3)_2$), 1.1 (br s, 6H, $CH(CH_3)_2$), 1.17 (dd overlapping with a broad signal at 1.2, 6H, J = 7.4, 12.7 Hz, $CH(CH_3)_2$), 1.2 (br s, 6H, $CH(CH_3)_2$), 1.42 (br s) and 1.54 (br s) and 1.74 (br m) (total 14H, overlapping signals of COE, CH_2 and $CH(CH_3)_2$ according to C−H correlation and COSY), 2.25 (d, 2H, $^{2}J_{PH}$ = 7.2 Hz, CH_2P), 2.46 (br m, 2H, COE,CH_2), 3.23 (br s, 1H, CHP), 3.85 (very br s, 2H, COE, CH═CH), 5.39 (br m, 1H, Py-CH), 6.47−6.54 (m, 2H, Py-CH). $^{13}C\{^{1}H\}$ NMR (126 MHz, toluene-d_8, 223 K): 17.34 (br s, $CH(CH_3)_2$), 17.91 (br s, $CH(CH_3)_2$), 18.64 (br s, $CH(CH_3)_2$), 20.07 (br s, $CH(CH_3)_2$), 25.5 (very br m, $CH(CH_3)_2$), 27.03 (br s, COE, CH_2), 32.26 (br s, COE, CH_2), 35.5 (br d, $^{2}J_{PC}$ = 18.2 Hz, CH_2P and COE-CH_2 according to C−H correlation), 62.22 (br d, $^{1}J_{PC}$ = 57 Hz, CHP), 63.6 (br s, COE, CH═CH), 96.5 (br m, Py-CH), 114.28 (br d, $^{3}J_{PC}$ = 18 Hz, Py-CH), 132.3 (br s, Py-CH), 158.6 (br m, Py-C), 173.5 (br m, Py-C). Acceptable elemental analysis results for **9** could not be obtained. The NMR spectrum of **9** appears in the Supporting Information.

[(PNN)Rh(NHC_6H_5)] (10). Method A: [(PNN*)RhN_2] (**5**) (15.0 mg, 0.033 mmol) was placed in an NMR tube, and a benzene-d_6 (or THF) solution (0.5 mL) of aniline (3 μL, 0.033 mmol) was added. The NMR tube was heated in an oil bath at 60 °C overnight, during which the color changed from red to brown, and complex **10** was obtained in quantitative yield according to a $^{31}P\{^{1}H\}$ NMR spectrum.[57]

Method B: To a THF (5 mL) suspension of complex **17** (39.7 mg, 0.065 mmol) was added ^{t}BuOK (7.3 mg, 0.065 mmol) in THF (5 mL), and a clear dark brown solution was immediately obtained. The reaction mixture was stirred at ambient temperature for 2 h, after which the solvent was removed by vacuum. The residue was extracted with benzene. The extracts were combined and filtered through a 0.2 μm Teflon filter, and the solvent was removed under vacuum to give complex **10** as a brown solid in 83% (28.1 mg) yield.

$^{31}P\{^{1}H\}$ NMR (121 MHz, benzene-d_6): 87.23 (d, $^{1}J_{RhP}$ = 220.4 Hz). ^{1}H NMR (300 MHz, benzene-d_6): 1.19 (t, 6H, $^{3}J_{HH}$ = 7.1 Hz, CH_3CH_2N), 1.31 (d, 18H, $^{3}J_{HP}$ = 12.5 Hz, $(CH_3)_3CP$), 2.07 (br s, 1H, Rh-NH), 2.28 (d, 2H, $^{2}J_{HP}$ = 8.3 Hz, CH_2P), 2.56−2.68 (m, 2H, CH_3CH_2N), 3.01 (m, 2H, CH_3CH_2N), 3.10 (s, 2H, Py-CH_2N), 6.01 (d, 1H, $^{3}J_{HH}$ = 7.6 Hz, Py-CH), 6.31 (d, 1H, $^{3}J_{HH}$ = 7.7 Hz, Py-CH), 6.46 (t, 1H, $^{3}J_{HH}$ = 7.0 Hz, anil-CH), 6.95 (t, 1H, $^{3}J_{HH}$ = 7.6 Hz, Py-CH), 7.01 (d, 2H, $^{3}J_{HH}$ = 7.7 Hz, anil-CH), 7.28 (t, 2H, $^{3}J_{HH}$ = 7.6 Hz, anil-CH). $^{13}C\{^{1}H\}$ NMR (125) MHz, benzene-d_6): 11.34 (s, CH_3CH_2N), 29.41 (d, $^{2}J_{CP}$ = 5.8 Hz, $(CH_3)_3CP$), 34.63 (dd, $^{1}J_{CP}$ = 13.0, $^{2}J_{CRh}$ = 2.5 Hz, $(CH_3)_3CP$), 36.48 (d, $^{1}J_{CP}$ = 17.0 Hz, CH_2P), 52.87 (br d or two overlapping singlets, in case of a doublet J = 1.7 Hz, CH_3CH_2N), 63.53 (d, J = 2.1 Hz, Py-CH_2N), 107.22 (s, anil-CH), 116.13 (s, anil-CH), 117.47 (s, Py-CH), 119.82 (d, $^{3}J_{CP}$ = 9.3 Hz, Py-CH), 127.39 (s, Py-CH), 128.86 (s, anil-CH), 160.50 (s, anil-C or Py-C), 160.55−160.62 (m, Py-C), 163.21 (s, anil-C or Py-C). Acceptable elemental analysis results for **10** could not be obtained. The NMR spectrum of **10** appears in the Supporting Information

[(PNN)Rh(*o*-Br-NHC_6H_4)] (11). Complex **11** was synthesized in the same manner as complex **10** by method A with complex **5** (15.0 mg, 0.033 mmol) and *o*-bromoaniline (4 μL, 0.035 mmol). The reaction mixture was heated overnight at 60 °C, during which the color changed from red to brown, and complex **11** was obtained in quantitative yield according to $^{31}P\{^{1}H\}$ NMR.

$^{31}P\{^{1}H\}$ NMR (121 MHz, benzene-d_6): 87.33 (d, $^{1}J_{RhP}$ = 208.8 Hz). ^{1}H NMR (400 MHz, benzene-d_6): 1.18 (br t, 6H, $^{3}J_{HH}$ = 7.0 Hz, CH_3CH_2N), 1.30 (18H, $^{3}J_{HP}$ = 12.6 Hz, $(CH_3)_3CP$), 2.28 (d, 2H, $^{2}J_{HP}$ = 8.4 Hz, CH_2P), 2.44−2.60 (br m, 2H, CH_3CH_2N), 2.82−2.96 (br m,

2H, CH_3CH_2N), 2.99 (br s, 1H, RhNH), 3.07 (s, 2H, Py-CH_2N), 6.01 (br d, 1H, $^3J_{HH}$ = 7.6 Hz, Py-CH), 6.15 (ddd, 1H, $^3J_{HH}$ = 6.8, 7.7 Hz, $^4J_{HH}$ = 1.7, anil-CH), 6.30 (br d, 1H, $^3J_{HH}$ = 7.6 Hz, Py-CH), 6.93 (br dt, 1H, $^3J_{HH}$ = 7.6 Hz, $^5J_{PH}$ = 0.8 Hz, Py-CH), 7.23 (m, 1H, anil-CH), 7.50 (dd, 1H, $^3J_{HH}$ = 8.2 Hz, $^4J_{HH}$ = 1.7, anil-CH), 7.56 (dd, 1H, $^3J_{HH}$ = 7.7 Hz, $^4J_{HH}$ = 1.6, anil-CH). $^{13}C\{^1H\}$ NMR (101 MHz, benzene-d_6): 11.37 (br s, CH_3CH_2N), 29.40 (d, $^2J_{CP}$ = 5.7 Hz, $(CH_3)_3CP$), 34.64 (dd, $^1J_{CP}$ = 13.2 Hz, $^2J_{CRh}$ = 2.4 Hz, $(CH_3)_3CP$), 36.40 (d, $^1J_{CP}$ = 17.3 Hz, CH_2P), 52.86 (br s, CH_3CH_2N), 63.50 (br d, J = 2.0 Hz, Py-CH_2N), 107.27 (s, anil-CH), 113.67 (br s, anil-CBr), 116.73 (s, anil-CH), 117.50 (s, Py-CH), 119.87 (d, $^3J_{CP}$ = 10.4 Hz, Py-CH), 127.83 (s, Py-CH), 127.93 (s, anil-CH), 131.87 (s, anil-CH), 158.11 (s, anil-CNH), 160.46 (s, Py-C), 160.72 (dd, J = 3.4, 6.3 Hz, Py-C). Acceptable elemental analysis results for **11** could not be obtained. The NMR spectrum of **11** appears in the Supporting Information.

[(PNN)Rh(*m*-Cl-*p*-Cl-NHC$_6$H$_3$)] (12). Complex **12** was synthesized in the same manner as complex **10** by method A with complex **5** (15.0 mg, 0.033 mmol) and *m*,*p*-dichloroaniline (5.3 mg, 0.033 mmol). The reaction mixture was heated for 3 h at 60 °C, during which the color changed from red to brown, and complex **12** was obtained in 97% yield by integration according to $^{31}P\{^1H\}$ NMR (another signal at 89.25 ppm ($^1J_{RhP}$ = 198.3 Hz) could be PNNRhCl). Crystals suitable for X-ray analysis were obtained from a concentrated solution of **12** in benzene by slow evaporation.

$^{31}P\{^1H\}$ NMR (121 MHz, benzene-d_6): 87.31 (d, $^1J_{RhP}$ = 216.7 Hz). ^1H NMR (500 MHz, benzene-d_6): 1.13 (t, 6H, $^3J_{HH}$ = 7.3 Hz, CH_3CH_2N), 1.23 (d, 18H, $^3J_{HP}$ = 12.5 Hz, $(CH_3)_3CP$), 2.17 (br s, Rh-N*H*-An), 2.26 (d, 2H, $^2J_{HP}$ = 8.5 Hz, CH_2P), 2.44−2.57 (m, 2H, CH_3CH_2N), 2.77−2.90 (m, 2H, CH_3CH_2N), 3.02 (s, 2H, Py-CH_2N), 5.80 (dd, 1H, $^3J_{HP}$ = 8.5 Hz, $^4J_{HP}$ = 2.5 Hz, An-CH), 6.01 (d, 1H, $^3J_{HP}$ = 8.0 Hz, Py-CH), 6.25 (d, 1H, $^4J_{HP}$ = 2.5 Hz, An-CH), 6.30 (d, 1H, $^3J_{HP}$ = 7.5 Hz, Py-CH), 6.89 (m, overlapping with a signal at 6.91, according to a C−H correlation and COSY, the signal was attributed to An-CH), 6.91 (m, overlapping with a signal at 6.91, according to a C−H correlation and COSY, the signal was attributed to Py-CH). $^{13}C\{^1H\}$ NMR (126 MHz, benzene-d_6): 11.30 (s, CH_3CH_2N), 29.29 (d, $^2J_{CP}$ = 5.8 Hz, $(CH_3)_3CP$), 34.55 (dd, $^1J_{CP}$ = 13.8 Hz, $^2J_{CRh}$ = 2.5 Hz $(CH_3)_3CP$), 36.27 (d, $^2J_{CP}$ = 17.6 Hz, CH_2P), 52.92 (br s, CH_3CH_2N), 63.41 (d, $^3J_{CP}$ = 2.0 Hz, Py-CH_2N), 114.36 (s, An-CH), 116.23 (s, An-CH), 117.51 (s, Py-CH), 119.82 (d, $^3J_{CP}$ = 10.2 Hz, Py-CH), 128.40 (s, Py-CH), 160.54 (br s, Py-C), 160.78 (dd, J = 2.5, 3.8 Hz, Py-C). Anal. for $C_{25}H_{39}Cl_2N_3PRh$: Calcd C, 51.21; H, 6.70. Found: C, 52.1; H, 6.75.

X-ray structural analysis of **12**. Crystal data: $C_{25}H_{39}Cl_2N_3PRh$, red prisms, 0.53 × 0.11 × 0.06 mm^3, orthorhombic, $P2_12_12_1$, a = 14.1476(5) Å, b = 24.9498(9) Å, c = 7.5796(3) Å, from 26 018 reflections, T = 120(2) K, V = 2675.45(17) Å^3, Z = 4, F_w = 586.37, D_c = 1.456 Mg/m^{-3}, μ = 0.916 mm^{-1}.

Data collection and processing: Bruker KappaApexII CCD diffractometer, Mo Kα (λ = 0.71073 Å), graphite monochromator, $-18 \le h \le 17$, $-33 \le k \le 33$, $-7 \le l \le 10$, $2\theta_{max}$ = 56.78, frame scan width = 0.5°, scan speed = 1.0° per 120 s, typical peak mosaicity 0.69°, 25 465 reflections collected, 7167 independent reflections (R_{int} = 0.0518). The data were processed with APEX2.

Solution and refinement: Structure solved by direct methods with Bruker AutoStructure. Full-matrix least-squares refinement based on F^2 with SHELXL-97. 330 parameters with no restraints, final R_1 = 0.0377 (based on F^2) for data with $I > 2\sigma(I)$, R_1 = 0.0429 on 6691 reflections, goodness-of-fit on F^2 = 1.034, largest electron density peak = 1.280 e Å^{-3}, and largest hole = −0.877 eÅ^3

[(PNN)Rh(*p*-NO$_2$−NHC$_6$H$_4$)] (13). Complex **13** was synthesized in the same manner as complex **10** by method A with complex **5** (30.4 mg, 0.067 mmol) and *p*-nitroaniline (9.2 mg, 0.067 mmol). The reaction mixture was heated for 3 h at 60 °C in THF, during which the color changed from red to deep brown. The solvent was removed under vacuum to give complex **13** as a dark brown solid in quantitative yield. Complex **13** has medium solubility in benzene and good solubility in THF.

$^{31}P\{^1H\}$ NMR (121 MHz, THF-d_8): 87.44 (d, $^1J_{RhP}$ = 216.4 Hz). ^1H NMR (400 MHz, THF-d_8): 1.30 (d, 18H, $^3J_{HP}$ = 12.8 Hz, $(CH_3)_3CP$), 1.38 (t, 6H, $^3J_{HH}$ = 6.7 Hz, CH_3CH_2N), 2.73−2.83 (m, 2H, CH_3CH_2N), 2.92 (d, 2H, $^2J_{HP}$ = 8.5 Hz, CH_2P, overlapping with the signal at 2.89−3.03), 2.89−3.03 (m, 2H, CH_3CH_2N), 3.95 (s, 2H, Py-CH_2N), 4.25 (s, 1H, RhNH), 5.91 (dd, 1H, $^3J_{HH}$ = 9.4 Hz, $^4J_{HH}$ = 2.5 Hz, anil-CH), 6.80 (dd, 1H, $^3J_{HH}$ = 9.5 Hz, $^4J_{HH}$ = 2.5 Hz, anil-CH), 6.93 (d, 1H, $^3J_{HH}$ = 7.7 Hz, Py-CH), 7.07 (d, 1H, $^3J_{HH}$ = 7.7 Hz, Py-CH), 7.37 (dd, 2H, $^3J_{HH}$ = 9.5 Hz, $^4J_{HH}$ = 2.5 Hz, anil-CH), 7.54 (dd, 1H, $^3J_{HH}$ = 7.7 Hz, $^5J_{PH}$ = 0.8 Hz, Py-CH), 7.64 (dd, 2H, $^3J_{HH}$ = 9.3 Hz, $^4J_{HH}$ = 2.6 Hz, anil-CH), 8.51 (dd, 2H, $^3J_{HH}$ = 9.5 Hz, $^4J_{HH}$ = 2.6 Hz, anil-CH). $^{13}C\{^1H\}$ NMR (101) MHz, THF-d_8): 11.60 (s, CH_3CH_2N), 29.80 (d, $^2J_{CP}$ = 5.6 Hz, $(CH_3)_3CP$), 35.46 (dd, $^1J_{CP}$ = 14.1 Hz, $^2J_{CRh}$ = 2.2 Hz, $(CH_3)_3CP$), 36.85 (d, $^1J_{CP}$ = 19.3 Hz, CH_2P), 53.98 (br s, CH_3CH_2N), 64.48 (br d, J = 1.8 Hz, Py-CH_2N), 116.21 (s, anil-CH), 116.56 (s, anil-CH), 119.98 (s, Py-CH), 121.24 (d, $^3J_{CP}$ = 10.8 Hz, Py-CH), 125.84 (s, anil-CH), 127.76 (s, anil-CH), 130.26 (s, anil-C), 132.01 (s, Py-CH), 161.89 (s, anil-C or Py-C), 162.44 (br dd, J = 3.6, 6.2 Hz, Py-C), 168.20 (s, anil-C or Py-C). Anal. for $C_{25}H_{40}N_4O_2PRh$: Calcd C, 53.38; H, 7.17. Found: C, 53.10; H, 7.13.

[(^{i}PrPNP)Rh(NHC$_6$H$_5$)] (14). Method A: [(^{i}PrPNP*)Rh(COE)] (**9**) (15.0 mg, 0.027 mmol) was placed in an NMR tube, and a benzene-d_6 (or THF) solution (0.5 mL) of aniline (9 μL, 0.099 mmol) was added. The NMR tube was heated in an oil bath at 60 °C overnight, during which the color changed from red to brown, and complex **14** was obtained in quantitative yield according to $^{31}P\{^1H\}$ NMR. The reaction of complex **7** with 1.2 equiv of aniline under the same conditions was sluggish, and for full conversion, a large excess of aniline is required.

Method B: To a THF (5 mL) suspension of complex **17** (23.7 mg, 0.038 mmol) was added ^{t}BuOK (4.2 mg, 0.038 mmol) in THF (5 mL), and a clear dark brown solution was immediately obtained. The reaction mixture was stirred at ambient temperature for 2 h, after which the solvent was removed by vacuum. The residue was extracted with benzene. The extracts were combined and filtered through a 0.2 μm Teflon filter, and the solvent was removed under vacuum to give complex **14** as a brown solid in 89% (18.2 mg) yield.

$^{31}P\{^1H\}$ NMR (121 MHz, benzene-d_6): 45.35 (d, $^1J_{RhP}$ = 156.7 Hz). ^1H NMR (500 MHz, benzene-d_6): 1.02 (q, 12 H, $^3J_{PH}$ = $^3J_{HH}$ = 6.7 Hz, $(CH_3)_2CH$), 1.23 (dd, 12H, $^3J_{PH}$ = 8.0 Hz, $^3J_{HH}$ = 7.4 Hz, $(CH_3)_2CH$), 1.85−1.97 (m, 4H, $(CH_3)_2CH$), 1.87 (overlapping with $(CH_3)_2CH$ signal, appears as a broad singlet in the SST experiment upon irradiation of CH_2P signal, Rh-NH), 2.47 (vt, 4H, J_{PH} = 3.4 Hz, CH_2P), 6.31 (d, 2H, $^3J_{HH}$ = 7.6 Hz, Py-CH), 6.46 (br t, 1H, $^3J_{HH}$ = 6.9 Hz, anil-CH), 6.86 (m, (overlapping with asignal at 6.88), 2H, anil-CH), 6.88 (m, (overlapping with a signal at 6.86), 1H, Py-CH), 7.26 (dd, 2H, J_{HH} = 1.0, 7.1 Hz, anil-CH). $^{13}C\{^1H\}$ NMR (126 MHz, benzene-d_6): 18.04 (s, $(CH_3)_2CH$), 19.02 (vt, J_{PC} = 3.7 Hz, $(CH_3)_2CH$), 24.94 (d vt, $^2J_{RhC}$ = 1.6 Hz, J_{PC} = 8.8 Hz, $(CH_3)_2CH$), 35.67 (vt, J_{PC} = 6.4 Hz, CH_2P), 107.46 (s, anil-CH), 116.47 (s, anil-CH), 119.49 (t, J_{PC} = 4.8 Hz, Py-CH), 128.44 (s, anil-CH), 129.47 (s, Py-CH), 163.60 (d vt, $^2J_{RhC}$ = 0.7 Hz, J_{PC} = 6.0 Hz, Py-C), 164.71 (br s, anil-C). Acceptable elemental analysis results for **14** could not be obtained. The NMR spectrum of **14** appears in the Supporting Information.

[(^{i}PrPNP)Rh(*p*-NO$_2$−NHC$_6$H$_4$)] (15). Complex **15** was synthesized in the same manner as complex **10** by method A with complex **7** (15 mg, 0.032 mmol) and *p*-nitroaniline (4.4 mg, 0.032 mmol). The reaction mixture was heated for 1 h at 60 °C, during which the color changed from red to deep purple. The solvent was removed by vacuum to give a dark brown solid as complex **15** in quantitative yield. Complex **15** has medium solubility in benzene and good solubility in THF.

$^{31}P\{^1H\}$ NMR (121 MHz, benzene-d_6): 46.87 (d, $^1J_{RhP}$ = 149.6 Hz). ^1H NMR (400 MHz, THF-d_8): 1.14−1.20 (m, 24 H, (according to $^1H\{^{31}P\}$: 1.17 (d, 12H, $^3J_{HH}$ = 6.9 Hz), 1.18 (d, 12H, $^3J_{HH}$ = 7.1 Hz), $(CH_3)_2CH$)), 2.09 (br quin. 4H, according to $^1H\{^{31}P\}$: sept. $^3J_{HH}$ = 7.0 Hz $(CH_3)_2CH$), 3.19 (vt, 4H, J_{PH} = 3.7 Hz, CH_2P), 4.47 (br s, 1H, Rh-NH), 5.86 (dd, 1H, J_{HH} = 2.5, 9.4, anil-CH), 7.09 (d, 2H, $^3J_{HH}$ =

7.7 Hz, Py-CH), 7.33 (dd, 1H, J_{HH} = 2.6, 9.4, anil-CH), 7.50 (t, 1H, $^3J_{HH}$ = 7.7 Hz, Py-CH), 6.56 (dd, 1H, J_{HH} = 2.5, 9.4, anil-CH), 7.64 (br dd, 1H, J_{HH} = 2.6, 9.4 Hz, anil-CH). $^{13}C\{^1H\}$ NMR (100 MHz, THF-d_8): 18.53 (br s, $(CH_3)_2CH$), 19.52 (vt, J_{PC} = 3.5 Hz, $(CH_3)_2CH$), 25.78 (d vt, J_{PC} = 9.4 Hz, $^2J_{RhC}$ = 1.4 Hz, $(CH_3)_2CH$), 36.02 (vt, J_{PC} = 7.6 Hz, CH_2P), 115.85 (s, anil-CH), 117.48 (s, anil-CH), 121.18 (vt, J_{PC} = 5.4 Hz, Py-CH), 125.49 (s, anil-CH), 127.73 (s, anil-CH), 130.15 (s, anil-C), 133.90 (s, Py-CH), 165.32 (br vt, J_{PC} = 5.4 Hz, Py-C), 168.36 (s, anil-C). Anal. for $C_{25}H_{40}N_3O_2PRh$: Calcd C, 51.82; H, 6.96. Found: C, 51.65; H, 6.90.

Spin Saturation Transfer (SST) Experiments. Spin saturation transfer experiments were performed on the anilide complexes **10** and **14** in benzene-d_6 and on the *p*-nitroanilide complexes **13** and **15** in THF-d_8 (0.02 M) and on the mixture of the anilide complexes with about a 5-fold excess of the corresponding free aniline. Each experiment involved selective spin saturation at the hydrogen atoms of the methylene benzylic arm (Py−CH_2−P). The response of the NH−anilide or NH_2−aniline signal was detected by comparison (difference spectrum) with a control experiment in which the sample was irradiated off-resonance under the same conditions. Using the SST technique, exchange between the benzylic protons Py−CH_2−P and the NH−anilide and between the benzylic protons Py−CH_2−P and NH_2−aniline was observed for complexes **10** and **14** only.

SST experiments were also preformed on complexes **5**−**7** and **9** (0.02 M) at 283 K in the presence of a 5-fold excess of aniline in toluene-d_8. $^{31}P\{^1H\}$ NMR spectra of the reaction mixtures performed prior to and after the SST experiments exhibits only signals of the starting complexes. Using the SST technique, exchange between the dearomatized benzylic arm Py−CH−P and the NH_2−aniline was observed.

[(PNN)Rh($NH_2C_6H_6$)][BF_4] (16). To a suspension of [(PNN)-RhN_2][BF_4] (**1**) (41.6 mg, 0.077 mmol) in THF (7 mL) in a Schlenk tube was added aniline (100 μL, 1.10 mmol), and the suspension was heated at 60 °C for 2 h. A clear orange solution was obtained, and the solvent volume was reduced to 1 mL by vacuum. Pentane was added to the THF solution, forming a precipitate, which was left standing overnight to allow easy decantation. After decantation, the light brown solid was washed with pentane (20 mL) and the solid was dried under vacuum to give the complex [(PNN)Rh($NH_2C_6H_5$)][BF_4] (**16**) in 84% yield (39.7 mg). Complex **16** has medium solubility in THF at ambient temperature, and it reacts readily with methylene chloride. It was found to be unstable in solution without a slight excess of aniline. The excess of aniline also improves the complex solubility in THF. When a solution of complex **16** was exposed to air, an unidentified green complex was obtained. Crystals suitable for X-ray analysis were obtained by addition of aniline (one drop) to a concentrated THF solution of **16** and layering with pentane.

$^{31}P\{^1H\}$ NMR (162 MHz, THF-d_8): 82.99 (d, $^1J_{RhP}$ = 197.1 Hz). ^1H NMR (400 MHz, THF-d_8): 1.35 (d, 18H, $^3J_{HP}$ = 12.8 Hz, $(CH_3)_3CP$), 1.43 (t, 6H, $^3J_{HH}$ = 7.1 Hz, CH_3CH_2N), 2.50 (dq (appears as q in $^1H\{^{31}P\}$ NMR), 4H, $^3J_{HH}$ = 7.1 Hz, $^4J_{PH}$ = 1.8 Hz, CH_3CH_2N), 3.06 (d, 2H, $^2J_{HP}$ = 9.0 Hz, CH_2P), 3.94 (s, 2H, Py-CH_2N), 4.93 (br s, 2H, Rh-NH_2), 6.98 (overlapping with free aniline signal, 1H, Py-CH), 7.11 (m, overlapping with signal at 7.13, 1H, anil-CH), 7.13 (m, overlapping with signal at 7.11, 1H, Py-CH), 7.25 (br t, 2H, $^3J_{HH}$ = 7.5 Hz, anil-CH), 7.55 (t, 2H, $^3J_{HH}$ = 7.7 Hz, Py-CH), 7.65 (d, 2H, $^3J_{HH}$ = 7.5 Hz, anil-CH). $^{13}C\{^1H\}$ NMR (101) MHz, THF-d_8): 12.20 (s, CH_3CH_2N), 29.52 (d, $^2J_{CP}$ = 5.4 Hz, $(CH_3)_3CP$), 35.29 (d, $^1J_{CP}$ = 15.1 Hz, $(CH_3)_3CP$), 36.61 (d, $^1J_{CP}$ = 22.1 Hz, CH_2P), 54.58 (br s, CH_3CH_2N), 64.36 (d, J = 1.6 Hz, Py-CH_2N), 118.64 (s, Py-CH), 120.87 (d, $^3J_{CP}$ = 10.7 Hz, Py-CH), 125.04 (s, anil-CH), 125.85 (s, anil-CH), 129.25 (s, anil-CH), 133.86 (s, Py-CH), 144.65 (s, anil-C), 162.84 (s, Py-C), 162.8 (m, Py-C). Acceptable elemental analysis results for **16** could not be obtained. The NMR spectrum of **16** appears in the Supporting Information.

X-ray structural analysis of **16**. Crystal data: $C_{25}H_{42}N_3PRh$ + BF_4, orange plate, 0.15 × 0.15 × 0.05 mm^3, triclinic, *P-1*, a = 10.6386(2) Å, b = 15.1960(2) Å, c = 18.7985(3) Å, α = 74.9166(7)°, β = 84.3107(7)°, γ = 72.6717(6)° from 12 761 reflections, T = 120(2) K, V = 2800.39(8) Å^3, Z = 4, F_w = 605.31, D_c = 1.436 Mg/m^{-3}, μ = 0.712 mm^{-1}.

Data collection and processing: Nonius KappaCCD diffractometer, Mo Kα (λ = 0.71073 Å), graphite monochromator; $-13 \le h \le 13$, $-19 \le k \le 19$, $-24 \le l \le 24$, frame scan width = 1.0°, scan speed = 1.0° per 20 s, typical peak mosaicity 0.768°, 69895 reflections collected, 12 844 independent reflections (R_{int} = 0.1109). The data were processed with HKL2000.

Solution and refinement: Structure solved by direct methods with SIR-92. Full-matrix least-squares refinement based on F^2 with SHELXL-97. 663 parameters with no restraints, final R_1 = 0.0526 (based on F^2) for data with $I > 2\sigma(I)$, R_1 = 0.0769 on 12 838 reflections, goodness-of-fit on F^2 = 1.104, largest electron density peak = 2.632 e Å^{-3}, and hole = −1.725 e Å^{-3}.

[(^{i}PrPNP)Rh($NH_2C_6H_5$)][BF_4] (17). To a suspension of [(^{i}PrPNP)-Rh(COE)][BF_4] (**8**) (31.0 mg, 0.048 mmol) in THF (7 mL) in a Schlenk tube was added aniline (100 μL, 1.10 mmol), and the reaction was heated at 60 °C for 4 h. A clear orange solution was obtained, and the THF volume was reduced to 1 mL by vacuum. Pentane was added to the THF solution, and a precipitate was formed. The precipitate was left overnight with the pentane to allow easy decantation. After decantation, the light brown solid was washed with pentane (20 mL) and the solid was dried under vacuum to give the complex [(^{i}PrPNP)Rh($NH_2C_6H_5$)][BF_4] (**17**) in 96% yield (28.3 mg). Crystals suitable for X-ray analysis were obtained by layering a concentrated THF solution of **17** with pentane.

$^{31}P\{^1H\}$ NMR (162 MHz, THF-d_8): 49.29 (d, $^1J_{RhP}$ = 135.7 Hz). ^1H NMR (400 MHz, THF-d_8): 1.09 (q, 12 H, $^3J_{HH}$ = $^3J_{PH}$ = 6.9 Hz, $(CH_3)_2CH$), 1.24 (dd apears as q, 12H, $^3J_{HH}$ = 7.2 Hz, $^3J_{PH}$ = 8.9 Hz, $(CH_3)_2CH$), 1.98−2.09 (m, 4H, according to $^1H\{^{31}P\}$: sept. $^3J_{HH}$ = 7.0 Hz, $(CH_3)_2CH$), 3.29 (vt, 4H, J_{PH} = 3.9 Hz, CH_2P), 5.27 (br s, 2H, Rh-NH_2), 7.17 (t, 1H, $^3J_{HH}$ = 7.7 Hz, Py-CH), 7.20 (d, 2H, $^3J_{HH}$ = 7.7 Hz, Py-CH), 7.30 (br d, 1H, $^3J_{HH}$ = 8 Hz, anil-CH), 6.99 (tt, 1H, $^3J_{HH}$ = 7.4 Hz, $^4J_{HH}$ = 1.1 Hz, anil-CH), 7.53 (br t, 1H, $^3J_{HH}$ = 7.7 Hz, anil-CH). $^{13}C\{^1H\}$ NMR (101 MHz, THF-d_8): 17.94 (s, $(CH_3)_2CH$), 19.31 (vt, J_{PC} = 3.5 Hz, $(CH_3)_2CH$), 24.66 (vt, J_{PC} = 10.2 Hz, $(CH_3)_2CH$), 35.14 (vt, J_{PC} = 8.9 Hz, CH_2P), 121.18 (vt, J_{PC} = 5.2 Hz, Py-CH), 123.91 (s, anil-CH), 125.17 (s, anil-CH), 129.17 (s, Py-CH), 135.19 (s, anil-CH), 148.24 (s, anil-C), 165.32 (br vt, J_{PC} = 5.4 Hz, Py-C). Anal. for $C_{25}H_{42}BF_4N_2P_2Rh$: Calcd C, 48.25; H, 6.80. Found: C, 48.38; H, 6.84.

X-ray structural analysis of **17**. Crystal data: $C_{25}H_{42}N_2P_2Rh$ + BF_4, orange needle, 0.16 × 0.01 × 0.01 mm^3, monoclinic, $P2_1/n$, a = 11.5987(4) Å, b = 21.1484(7) Å, c = 11.7603(4) Å, β = 102.226(1)° from 18° of data, T = 120(2) K, V = 2819.30(17) Å^3, Z = 4, F_w = 622.27, D_c = 1.466 Mg/m^{-3}, μ = 0.763 mm^{-1}.

Data collection and processing: Bruker KappaApexII CCD diffractometer, Mo Kα (λ = 0.71073 Å), graphite monochromator; Miracol optics, $-16 \le h \le 14$, $-29 \le k \le 26$, $-16 \le l \le 16$, 2θ max = 60.50°, frame scan width = 0.5°, scan speed = 1.0° per 160 s, typical peak mosaicity 0.79°, 30 707 reflections collected, 8359 independent reflections (R_{int} = 0.034). The data were processed with the BrukerApex2 package.

Solution and refinement: Structure solved by direct methods with Bruker AutoStructure. Full-matrix least-squares refinement based on F^2 with SHELXL-97. 330 parameters with no restraints, final R_1 = 0.0288 (based on F^2) for data with $I > 2\sigma(I)$, R_1 = 0.0454 on 8359 reflections, goodness-of-fit on F^2 = 1.015, largest electron density peak = 0.869 e Å^{-3}, and hole = −0.332 e Å^{-3}.

Treatment of Complexes 10 and 14 with *p*-Nitroaniline. A 7.0 mg (0.017 mmol) portion of **10** was placed in an NMR tube and dissolved in a 0.5 mL THF solution of *p*-nitroaniline (0.034 M, 0.017 mmol). The NMR tube was shaken to give a clear solution and placed in an oil bath and heated to 60 °C for 20 h. The same procedure was performed with complex **14** (9.3 mg, 0.017 mmol). The progress of the reactions was monitored by $^{31}P\{^1H\}$ NMR after 1, 4, and 18 h, which revealed for both **10** and **14** 45% conversion to complexes **13** and **15**, respectively, after 1 h, 80% conversion after 4 h, and full conversion after 18 h. Free aniline in the reactions mixture was detected by GCMS.

Treatment of Complexes 10 and 13−15 with CO. A benzene-d_6 solution of **10** (10.0 mg, 0.019 mmol) was placed in a J. Young NMR tube and cooled to −196 °C, and the nitrogen atmosphere was replaced by CO. The reaction mixture was slowly warmed to room temperature, and the solution color changed from brown to red. According to $^{31}P\{^1H\}$ NMR, ^1H NMR, and GCMS, complex **18** and the corresponding aniline were obtained in quantitative yield. Complexes **13**, **14**, and **15** were reacted in the same maner as **10** to give complexes **18** and **19**, respectively, along with the corresponding free aniline.

Treatment of Complexes 14 and 15 with PEt_3. A benzene-d_6 solution of **14** (7.6 mg, 0.014 mmol) was placed in a J. Young NMR tube, and 0.05 mL of PEt3 (0.339 mmol) was added. The NMR tube was placed in an oil bath and heated to 60 °C for 12 h, during which the color turned from brown to red, and complex **22** was obtained in quantitative yield along with free aniline according to $^{31}P\{^1H\}$ NMR, ^1H NMR, and GCMS. Complex **15** (8.5 mg, 0.015 mmol) was reacted in the same manner as **14** in THF with PEt_3 (0.05 mL, 0.339 mmol) to give complex **22** and *p*-nitroaniline in quantitative yield.

[(PNN*)Rh(CO)] (18). Method A: A benzene solution (7 mL) of [(PNN*)RhN$_2$] (**5**) (15 mg, 0.033 mmol) in a Schlenk tube was cooled to −196 °C, and the nitrogen atmosphere was replaced by CO. The reaction mixture was slowly warmed to room temperature, and the solution color changed from dark red to red (minor change). The solvent was removed under vacuum to give complex **18** as a red solid in quantitative yield. Method B: To a THF (3 mL) suspension of [(PNN)Rh(CO)][BF$_4$] (**20**) (21.0 mg, 0.04 mmol) was added a THF (3 mL) solution of ^{t}BuOK (4.5 mg, 0.04 mmol), and the reaction mixture turned to a clear red solution. The solution was stirred at ambient temperature for 2 h (or until most of the yellow solid (complex **20**) disappeared), and the solvent was removed under vacuum. The residue was extracted with benzene. The extracts were combined and filtered through a 0.2 μm Teflon filter, and the solvent was removed under vacuum, resulting in complex **18** as a red solid in 90% (16.3 mg) yield.

$^{31}P\{^1H\}$ NMR (162 MHz, benzene-d_6): 90.88 (d, $^1J_{RhP}$ = 156.6 Hz). ^1H NMR (400 MHz, benzene-d_6): 1.16 (t, 6H, $^3J_{HH}$ = 7.1 Hz, CH_3CH_2N), 1.45 (d, 18H, $^3J_{PH}$ = 13.5 Hz, $(CH_3)_3CP$), 2.28−3.39 (m, 2H, CH_3CH_2N), 2.40−2.51 (m, 2H, CH_3CH_2N), 2.94 (br s, 2H, Py-CH_2N), 3.44 (br s, 1H, CHP), 5.14 (d, 1H, $^3J_{HH}$ = 6.6 Hz, Py-H), 6.27 (d, 1H, $^3J_{HH}$ = 8.6 Hz, Py-H), 6.39−6.46 (m, 2H, Py-H). $^{13}C\{^1H\}$ NMR 101 MHz, benzene-d_6): 12.69 (s, CH_3CH_2N), 29.74 (br d, $^2J_{CP}$ = 3.2 Hz, $(CH_3)_3CP$), 36.50 (d, $^1J_{CP}$ = 26.7 Hz, $(CH_3)_3CP$), 54.85 (s, CH_3CH_2N), 63.12 (d, $^1J_{CP}$ = 56.0 Hz, CHP), 64.11 (s, Py-CH_2N), 95.85 (s, Py-CH), 113.43 (d, $^3J_{CP}$ = 23.2 Hz, Py-CH), 132.56 (s, Py-CH), 119.82 (d, $^3J_{CP}$ = 9.3 Hz, Py-CH), 127.39 (s, Py-CH), 157.66 (br s, Py-C), 168.71−169.04 (m, Py-C), 195.57−196.56 (br d, $^1J_{RhC}$ = 57 Hz, CO). IR(ν_{CO}) = 1939.0 cm^{-1}. Anal. for $C_{20}H_{34}N_2OPRh$: Calcd C, 53.10; H, 7.58. Found: C, 52.64; H, 7.64.

[(^{i}PrPNP*)Rh(CO)] (19). Complex **19** was synthesized in the same manner as complex **18**. Method A: Reaction of [(^{i}PrPNP*)Rh(C_2H_4)] (**7**) (15 mg, 0.032 mmol) resulted in quantitative yield of complex **19** as a red solid. Method B: Reaction of [(^{i}PrPNP)Rh(CO)][BF$_4$] (**21**) with ^{t}BuOK resulted in complex **19** in quantitative yield.

$^{31}P\{^1H\}$ NMR (202 MHz, benzene-d_6): AB system centered at 61.41 (dd, $^1J_{RhP}$ = 123.5 Hz, $^2J_{PP}$ = 249.0 Hz) and 58.30 (dd, $^1J_{RhP}$ = 123.5 Hz, $^2J_{PP}$ = 249.0 Hz). ^1H NMR (500 MHz, benzene-d_6): 0.81 (dd, 6H, $^3J_{PH}$ = 13.5 Hz, $^3J_{HH}$ = 7.0 Hz, $(CH_3)_2CH$), 1.00 (dd, 6H, $^3J_{PH}$ = 16.2 Hz, $^3J_{HH}$ = 7.1 Hz, $(CH_3)_2CH$), 1.22 (dd, 6H, $^3J_{PH}$ = 14.0 Hz, $^3J_{HH}$ = 6.8 Hz, $(CH_3)_2CH$), 1.35 (dd, 6H, $^3J_{PH}$ = 16.3 Hz, $^3J_{HH}$ = 7.0 Hz, $(CH_3)_2CH$), 1.60 (m, 2H, in $^1H\{^{31}P\}$ NMR appears as hep. $^3J_{HH}$ = 7.0 Hz, $(CH_3)_2CH$), 2.06 (d hep., 2H, in $^1H\{^{31}P\}$ NMR appears as hep. $^3J_{HH}$ = 7.0 Hz, J_{PH} = 2.6 Hz, $(CH_3)_2CH$), 2.53 (d, 2H, $^2J_{PH}$ = 9.5 Hz, CH_2P), 3.45 (d, 1H, $^2J_{PH}$ = 4.4 Hz, CHP), 5.35 (d, 1H, $^3J_{HH}$ = 6.0 Hz, Py-CH), 6.39−6.45 (m, 2H, Py-CH). $^{13}C\{^1H\}$ NMR (125 MHz, benzene-d_6): 18.10 (s, $(CH_3)_2CH$), 18.28 (s, $(CH_3)_2CH$), 19.27 (d, $^2J_{PC}$ = 5.5 Hz, $(CH_3)_2CH$), 19.99 (d, $^2J_{PC}$ = 5.6 Hz, $(CH_3)_2CH$), 25.02 (d vt, $^2J_{RhC}$ = $^3J_{PC}$ = 2.1 Hz, $^1J_{PC}$ = 21.3 Hz, $(CH_3)_2CH$), 26.46 (d vt, $^2J_{RhC}$ = $^3J_{PC}$ = 2.2 Hz, $^1J_{PC}$ = 29.3 Hz, $(CH_3)_2CH$), 34.78 (d, $^1J_{PC}$ = 18.6 Hz, CH_2P), 61.48 (dd, J = 2.0 Hz, $^1J_{PC}$ = 51.8 Hz, CHP), 97.87 (d, $^3J_{PC}$ = 11.7 Hz, Py-CH), 114.43 (d, $^3J_{PC}$ = 19.0 Hz, Py-CH), 132.54 (vt, J = 1.5 Hz, Py-CH), 159.35 (ddd, J = 1.8, 3.7 Hz, $^2J_{PC}$ = 8.5 Hz, Py-C), 174.10 (ddd, J = 2.4, 4.7 Hz, $^2J_{PC}$ = 20.7 Hz, Py-C), 197.90 (dt, $^1J_{RhC}$ = 65.7 Hz, $^2J_{PC}$ = 13.3 Hz, CO). IR(ν_{CO}) = 1954.2 cm^{-1}. Anal. for $C_{20}H_{34}NOP_2Rh$: Calcd C, 51.18; H, 7.30. Found: C, 50.41; H, 7.33.

[(PNN)Rh(CO)][BF$_4$] (20). An acetone solution (7 mL) of complex **1** (15 mg, 0.028 mmol) in a Schlenk tube was cooled to −196 °C, and the nitrogen atmosphere was replaced by CO. The reaction mixture was slowly warmed to room temperature to give a bright yellow solution. The solvent was removed under vacuum, and the obtained solid was washed with pentane (10 mL) and dried again under vacuum to give complex **20** as a yellow solid in quantitative yield. $^{31}P\{^1H\}$ NMR (121 MHz, acetone-d_6): 98.18 (d, $^1J_{RhP}$ = 149.4 Hz). ^1H NMR (400 MHz, acetone-d_6): 1.42 (d, 18H, $^3J_{PH}$ = 14.8 Hz, $(CH_3)_3CP$), 1.60 (t, 6H, $^3J_{HH}$ = 7.1 Hz, CH_3CH_2N), 3.10−3.19 (m, 2H, CH_3CH_2N), 3.31−3.40 (m, 2H, CH_3CH_2N), 4.07 (d, $^2J_{PH}$ = 9.6 Hz, 2H, CH_2P), 4.57 (br s, 2H, Py-CH_2N), 7.59 (d, 1H, $^3J_{HH}$ = 7.9 Hz, Py-H), 6.27 (d, 1H, $^3J_{HH}$ = 7.9 Hz, Py-H), 8.05 (dt, J = 0.9, $^3J_{HH}$ = 7.9 Hz, 2H, Py-H). $^{13}C\{^1H\}$ NMR (101 MHz, acetone-d_6): 13.29 (s, CH_3CH_2N), 28.90 (d, $^2J_{CP}$ = 4.3 Hz, $(CH_3)_3CP$), 36.09 (d, $^1J_{CP}$ = 23.2 Hz, CH_2P), 36.30 (dd, $^1J_{CP}$ = 21.8 Hz, $^2J_{CRh}$ = 1.8 Hz, $(CH_3)_3CP$), 56.84 (br d, J = 1.9 Hz, CH_3CH_2N), 54.68 (br d, J = 1.4 Hz, Py-CH_2N), 120.61 (s, Py-CH), 122.58 (d, $^3J_{CP}$ = 10.7 Hz, Py-CH), 141.39 (s, Py-CH), 162.98 (br d, J = 1.9 Hz, Py-C), 163.26−163.34 (m, Py-C), 193.15 (dd, $^1J_{RhC}$ = 73.7 Hz, $^2J_{CP}$ = 16.8 Hz, CO). IR(ν_{CO}) = 1965.8 cm^{-1}. Anal. for $C_{20}H_{35}BF_4N_2OPRh$: Calcd C, 44.47; H, 6.53. Found: C, 44.62; H, 6.61.

[(^{i}PrPNP)Rh(CO)][BF$_4$] (21). Complex **21** was synthesized in the same manner as complex **20** from [(^{i}PrPNP)Rh(COE)][BF$_4$] (**8**) or [(^{i}PrPNP)Rh(C_2H_4)][BF$_4$] (**4**). When complex **8** was used, further washing of the obtained solid with pentane (20 mL) was required in order to remove free COE. Complex **21** was obtained as a yellow solid in quantitative yield.

Complex **21** dissolves well in acetone and methylene chloride and is stable in methylene chloride, whereas in acetone-d_6, fast H−D exchange with the benzylic arms was observed. Because of the H−D exchange in acetone-d_6, the CH_2−P signal was observed as a very broad multiplet in the ^1H NMR and was not observed in the $^{13}C\{^1H\}$NMR. The $^{31}P\{^1H\}$ NMR of the complex in acetone-d_6 appears as a doublet of multiplets.

$^{31}P\{^1H\}$ NMR (121 MHz, acetone-d_6): 65.93 (d of multiplet, $^1J_{RhP}$ = 119.4 Hz). $^{31}P\{^1H\}$ NMR (202 MHz, methylene chloride-d_2): 64.73 (d, $^1J_{RhP}$ = 119.4 Hz). ^1H NMR (300 MHz, acetone-d_6): 1.23 (dd, 12 H, $^3J_{PH}$ = 8.5 Hz, $^3J_{HH}$ = 7.0 Hz, $(CH_3)_2CH$), 1.34 (dd, 12H, $^3J_{PH}$ = 10.8 Hz, $^3J_{HH}$ = 7.0 Hz, $(CH_3)_2CH$), 2.47−2.60 (m, 4H, in $^1H\{^{31}P\}$ NMR appears as hep. $^3J_{HH}$ = 7.0 Hz, $(CH_3)_2CH$), 4.03−4.11 (br m, CHD-P), 7.72 (d, 2H, $^3J_{HH}$ = 7.8 Hz, Py-CH), 8.04 (t, 1H, $^3J_{HH}$ = 7.8 Hz, Py-CH). ^1H NMR (500 MHz, methylene chloride-d_2): 1.19 (dd, 12H, $^3J_{PH}$ = 8.5 Hz, $^3J_{HH}$ = 7.0 Hz, $(CH_3)_2CH$), 1.30 (dd, 12H, $^3J_{PH}$ = 10.5 Hz, $^3J_{HH}$ = 7.0 Hz, $(CH_3)_2CH$), 2.37−2.46 (m, 4H, in $^1H\{^{31}P\}$ NMR appears as hep. $^3J_{HH}$ = 7.0 Hz, $(CH_3)_2CH$), 3.76 (vt, 4H, J_{PH} = 4.0 Hz, CH_2P), 7.59 (d, 2H, $^3J_{HH}$ = 7.7 Hz, Py-CH), 7.90 (t, 1H, $^3J_{HH}$ = 7.7 Hz, Py-CH). $^{13}C\{^1H\}$ NMR (101 MHz, acetone-d_6): 18.42 (s, $(CH_3)_2CH$), 19.49 (br s, $(CH_3)_2CH$), 25.73 (m, $(CH_3)_2CH$), 122.92 (vt, J_{PC} = 5.6 Hz, Py-CH), 141.62 (s, Py-CH), 165.69 (br s, Py-C), 194.69 (dt, $^1J_{RhC}$ = 69.0, $^2J_{PC}$ = 14.0 Hz, RhCO). $^{13}C\{^1H\}$ NMR (125 MHz, methylene chloride-d_2): 18.33 (s, $(CH_3)_2CH$), 19.33 (vt, J_{PC} = 2.6 Hz $(CH_3)_2CH$), 25.56 (d vt, $^2J_{RhC}$ = 1.7 Hz, J_{PC} = 13.1 Hz, $(CH_3)_2CH$), 35.69 (vt, J_{PC} = 9.8 Hz, CH_2P), 122.50 (vt, J_{PC} = 5.6 Hz, Py-CH), 141.11 (s, Py-CH), 164.50 (d vt, $^2J_{RhC}$ = 1.6 Hz, J_{PC} = 5.7 Hz, Py-C), 193.40 (dt, $^1J_{RhC}$ = 69.0, $^2J_{PC}$ = 14.0 Hz, CO). IR(ν_{CO}) = 1976 cm^{-1}. Anal. for $C_{20}H_{35}BF_4NOP_2Rh$: Calcd C, 43.11; H, 6.33. Found: C, 43.98; H, 6.53.

[(^{i}PrPNP*)Rh(PEt_3)] (22). To a suspension of [(^{i}PrPNP)Rh(COE)][BF$_4$] **8** (22.5 mg, 0.035 mmol) in THF (3 mL) was added a drop of PEt_3 (about 15 mg, 0.13 mmol), and the reaction was stirred at ambient temperature for 30 min, during which a clear yellow solution was obtained. Pentane (17 mL) was added, and a yellow

precipitate was obtained, which was separated by decantation and washed with 20 mL of pentane. The yellow solid was dried under vacuum to give the complex [(^{i}PrPNP)Rh(PEt$_3$)][BF$_4$] (**23**) in 94% yield. To a THF solution (3 mL) of **23** (21.1 mg, 0.033 mmol) was added ^{t}BuOK (3.7 mg, 0.033 mmol) in THF (3 mL), and the solution color changed immediately from yellow to red. The reaction nixture was stirred at ambient temperature for 30 min, after which the solvent was removed under vacuum. The residue was extracted with benzene. The extracts were combined and filtered through a (0.2 μm) Teflon filter, and the solvent was removed under vacuum, resulting in complex **22** as a red solid in 91% (16.9 mg) yield.

^{31}P{^{1}H} NMR (202 MHz, benzene-d_6): ABX system centered at 50.18 (ddd, 1P, $^1J_{RhP}$ = 136.2 Hz, $^2J_{PPtrans}$ = 269.7 Hz, $^2J_{PPcis}$ = 37.7 Hz) and 43.95 (ddd, 1P, $^1J_{RhP}$ = 135.8 Hz, $^2J_{PPtrans}$ = 269.7 Hz, $^2J_{PPcis}$ = 40.2 Hz), 28.68 (br dt, 1P, $^1J_{RhP}$ = 155.9 Hz, $^2J_{PPcis}$ = 39 Hz). ^{1}H NMR (500 MHz, benzene-d_6): 0.95 (dd, 3H, $^3J_{HH}$ = 6.9 Hz, $^3J_{PH}$ = 5.1 Hz, P(CH$_2$C*H*$_3$)$_3$), 0.99−1.07 (m, overlapping with an impurity signal, should give a 6H signal, real intgration gives 14H signal, P(CH$_2$C*H*$_3$)$_3$), 1.28 (dd, 6H, $^3J_{HH}$ = 6.7 Hz, $^3J_{PH}$ = 5.1 Hz, (C*H*$_3$)$_2$CH), 1.39 (dd, 6H, $^3J_{HH}$ = 7.1 Hz, $^3J_{PH}$ = 8.3 Hz, (C*H*$_3$)$_2$CH), 1.53 (quin. 6H, $^2J_{PH}$ = $^3J_{HH}$ = 7.3 Hz, P(C*H*$_2$CH$_3$)$_3$), 1.64 (m, appeaprs as hept. in ^{1}H{^{31}P} NMR, $^3J_{HH}$ = 6.9 Hz, 2H, (CH$_3$)$_2$C*H*), 1.95 (m, appeaprs as hept. in ^{1}H{^{31}P} NMR, $^3J_{HH}$ = 6.9 Hz, 2H, (CH$_3$)$_2$C*H*), 2.61 (d, 2H, $^2J_{PH}$ = 9.0 Hz, CH$_2$P), 3.51 (d, 1H, $^2J_{PH}$ = 3.2 Hz, CHP), 5.54 (d, 1H, $^3J_{HH}$ = 6.2 Hz, Py-CH), 6.54 (br d, 1H, $^3J_{HH}$ = 8.6 Hz, Py-CH), 6.60 (m, 1H, Py-CH). ^{13}C{^{1}H} NMR (126 MHz, benzene-d_6): 18.23 (s, P(CH$_2$C*H*$_3$)$_3$), 18.64 (s, P-(CH$_2$C*H*$_3$)$_3$), 19.50 (d, $^2J_{PC}$ = 6.2 Hz, (C*H*$_3$)$_2$CH), 21.04 (d, $^2J_{PC}$ = 7.0 Hz, (C*H*$_3$)$_2$CH), 21.96 (br d, $^1J_{PC}$ = 23.7 Hz, P(C*H*$_2$CH$_3$)$_3$), 26.29 (d, $^1J_{PC}$ = 16.6 Hz, (CH$_3$)$_2$C*H*), 28.17 (d, $^1J_{PC}$ = 22.7 Hz, (CH$_3$)$_2$C*H*), 37.27 (dd, J = 3.5 Hz, $^1J_{PC}$ = 19.8 Hz, CH$_2$P), 61.93 (dd, J = 2.4 Hz, $^1J_{PC}$ = 51.8 Hz, CHP), 96.55 (d, $^3J_{PC}$ = 10.6 Hz, Py-CH), 112.58 (d, $^3J_{PC}$ = 18.1 Hz, Py-CH), 131.56 (br s, Py-CH), 158.35 (br d, $^2J_{PC}$ = 7 Hz, Py-C), 172.31 (d m, $^2J_{PC}$ = 21 Hz, Py-C). Anal. for C$_{25}$H$_{49}$NP$_3$Rh: Calcd C, 53.67; H, 8.83. Found: C, 53.43; H, 8.93.

[(^{i}PrPNP)Rh(PEt$_3$)][BF$_4$] (23). The synthesis of complex **23** is described above, under description of the synthesis of complex **22**.

^{31}P{^{1}H} NMR (202 MHz, acetone-d_6): 56.44 (dd, 2P, $^2J_{PP}$ = 39.3 Hz, $^1J_{PRh}$ = 134.9 Hz), 30.04 (dt, 1P, $^2J_{PP}$ = 39.3 Hz, $^1J_{PRh}$ = 155.6 Hz). ^{1}H NMR (500 MHz, acetone-d_6): 1.23 (dd appears as q, 12 H, $^3J_{PH}$ = $^3J_{HH}$ = 6.8 Hz, (C*H*$_3$)$_2$CH), 1.19 (dt, 9H, $^3J_{HH}$ = 7.5 Hz, $^3J_{PH}$ = 15.4 Hz, P(CH$_2$C*H*$_3$)$_3$), 1.34 (dd appears as q, 12H, $^3J_{PH}$ = 8.5 Hz, $^3J_{HH}$ = 7.2 Hz, (C*H*$_3$)$_2$CH), 1.81 (br quin., 6H, $^3J_{PH}$ = $^3J_{HH}$ = 7.5 Hz, in ^{1}H{^{31}P} appears as a dq with $^3J_{RhH}$ = 0.9 Hz, P(C*H*$_2$CH$_3$)$_3$), 2.33 (m, 4H, in ^{1}H{^{31}P} NMR appears as hep. $^3J_{HH}$ = 7.0 Hz, (CH$_3$)$_2$C*H*), 3.65 (vt, 4H, $^3J_{PH}$ = 3.7 Hz, P-CH$_2$), 7.57 (d, 2H, $^3J_{HH}$ = 7.7 Hz, Py-CH), 7.90 (t, 1H, $^3J_{HH}$ = 7.7 Hz, Py-CH). ^{13}C{^{1}H} NMR (125 MHz, acetone-d_6): 9.63 (s, P(CH$_2$C*H*$_3$)$_3$), 18.51 (s, (C*H*$_3$)$_2$CH), 19.53 (vt, J_{PC} = 2.6 Hz, (C*H*$_3$)$_2$CH), 21.69 (d of m, $^1J_{PC}$ = 28 Hz, P(C*H*$_2$CH$_3$)$_3$), 26.52 (d vt, $^3J_{PC}$ or $^2J_{RhC}$ = 2.1 Hz, J_{PC} = 10.9 Hz (CH$_3$)$_2$C*H*), 36.89 (d vt, J_{PC} = 9.8 Hz, $^3J_{PC}$ or $^2J_{RhC}$ = 2.4 Hz, CH$_2$P), 121.50 (d vt, J_{PC} = 4.5 Hz, $^3J_{RhC}$ = 1.1 Hz, Py-CH), 139.02 (s, Py-CH), 163.11 (vt, J_{PC} = 4.3 Hz, Py-C). Anal. for C$_{25}$H$_{50}$BF$_4$NP$_3$Rh: Calcd C, 46.39; H, 7.79. Found: C, 46.78; H, 7.74.

[(PNN*)Rh(*p*-NO$_2$-NHC$_6$H$_4$)][K] (24). To a THF solution (5 mL) of [(PNN)Rh(*p*-NO$_2$-NHC$_6$H$_4$)] **13** (10 mg, 0.018 mmol) was added ^{t}BuOK (2.0 mg, 0.018 mmol) in THF (5 mL), and the reaction color turned immediately from deep red to purple. According to the ^{31}P{^{1}H} spectrum, complex **13** was fully converted to complex **24**. Since complex **24** was not stable under vacuum, it was fully charcterized in situ by NMR. For charcterization, complex **13** was placed in an NMR tube and dissolved in a solution of ^{t}BuOK (2 mg, 0.018 mmol) in 0.5 mL of THF-d_8 and the NMR tube was shaken a few times.

^{31}P{^{1}H} NMR (121 MHz, THF-d_8): 80.09 (d, $^1J_{RhP}$ = 206.9 Hz). ^{1}H NMR (500 MHz, THF-d_8): 1.21 (d, $^3J_{PH}$ = 11.7 Hz, (C*H*$_3$)$_3$CP), 1.32 (t, $^3J_{HH}$ = 7.1 Hz, C*H*$_3$CH$_2$N), 2.66−2.83 (br m, 4H, CH$_3$C*H*$_2$N), 3.10 (br s, 1H, CHP), 3.46 (br s, 2H, Py-CH$_2$N), 5.00 (d, 1H, $^3J_{HH}$ = 6.5 Hz, Py-H), 5.68 (d, 1H, $^3J_{HH}$ = 8.7 Hz, Py-H), 5.89 (br d, $^3J_{HH}$ = 9.7 Hz, anil-CH), 6.10 (br t, 1H, $^3J_{HH}$ = 7.0 Hz, Py-H), 7.18 (br d, $^3J_{HH}$ = 9.8 Hz, anil-CH), 7.25 (br d, $^3J_{HH}$ = 9.9 Hz, anil-CH), 7.60 (br d, $^3J_{HH}$ = 9.7 Hz, anil-CH). ^{13}C{^{1}H} NMR (101 MHz, THF-d_8): 11.28 (s, *C*H$_3$CH$_2$N), 30.62 (d, $^2J_{CP}$ = 4.4 Hz, (*C*H$_3$)$_3$CP), 35.88 (dd, $^1J_{CP}$ = 18.1 Hz, $^2J_{CRh}$ = 1.7 Hz, (CH$_3$)$_3$CP), 52.78 (br s, CH$_3$*C*H$_2$N), 63.54 (d, $^1J_{CP}$ = 55.0 Hz, CHP), 64.89 (s, Py-CH$_2$N), 94.12 (s, Py-CH), 109.18 (d, $^3J_{CP}$ = 18.0 Hz, Py-CH), 120.43 (s, anil-CH), 122.62 (s, anil-CH), 123.46 (s, anil-CH), 126.29 (s, anil-CH), 128.06 (s, anil-C), 128.90 (s, Py-CH), 158.09 (br d, J = 1.2 Hz, C), 167.70 (s, C), 169.53 (m, Py-C). Acceptable elemental analysis results for **24** could not be obtained. The NMR spectrum of **24** appears in the Supporting Information.

[(^{i}PrPNP*)Rh(*p*-NO$_2$−NHC$_6$H$_4$)][K] (25). Complex **25** was prepared in the same manner as complex **24** from complex [(^{i}PrPNP)-Rh(*p*-NO$_2$−NHC$_6$H$_4$)] (**15**) (10 mg, 0.017 mmol). According to the ^{31}P{^{1}H} spectrum, complex **15** was fully converted to complex **25**.

^{31}P{^{1}H} NMR (202 MHz, THF-d_8): AB system centered at 46.07 (dd, $^1J_{RhP}$ = 150.5 Hz, $^2J_{PP}$ = 314.2 Hz) and 39.65 (dd, $^1J_{RhP}$ = 148.7 Hz, $^2J_{PP}$ = 314.2 Hz). ^{1}H NMR (500 MHz, THF-d_8): 1.20−1.29 (m, overlapping with ^{t}BuOH signal, (C*H*$_3$)$_2$CH), 1.77 (m, 2H, (CH$_3$)$_2$C*H*), 1.94 (m, 2H, (CH$_3$)$_2$C*H*), 2.73 (d, 2H, $^1J_{PH}$ = 8.4 Hz, C*H*$_2$P), 3.08 (d, $^1J_{PH}$ = 3.3 Hz, C*H*P), 5.18 (d, 1H, $^3J_{HH}$ = 6.5 Hz, Py-CH), 5.78 (d, 1H, $^3J_{HH}$ = 8.5 Hz, Py-CH), 5.91 (dd, 1H, J_{HH} = 2.0, 9.7 Hz, anil-CH), 6.08 (br t, 1H, $^3J_{HH}$ = 7.5 Hz, Py-CH), 6.98 (dd, 1H, J_{HH} = 2.0, 9.9, anil-CH), 7.24 (dd, 1H, J_{HH} = 2.0, 9.7, anil-CH). The Rh−NH signal was not detected. ^{13}C{^{1}H} NMR (126 MHz, THF-d_8): 18.51 (s, (*C*H$_3$)$_2$CH), 18.72 (s, (*C*H$_3$)$_2$CH), 19.68 (d, $^2J_{PC}$ = 7.4 Hz, (*C*H$_3$)$_2$CH), 20.06 (d, $^2J_{PC}$ = 7.6 Hz, (*C*H$_3$)$_2$CH), 25.75 (d, $^1J_{PC}$ = 14.9 Hz, (CH$_3$)$_2$C*H*), 26.67 (d, $^1J_{PC}$ = 21.33 Hz, (CH$_3$)$_2$C*H*), 36.15 (d, $^1J_{PC}$ = 17.7 Hz, C*H*$_2$P), 59.94 (d, $^1J_{PC}$ = 50.6 Hz, C*H*P), 96.77 (d, $^3J_{PC}$ = 11.2 Hz, Py-CH), 110.65 (d, $^3J_{PC}$ = 17.9 Hz, Py-CH), 119.50 (s, anil-CH), 123.24 (s, anil-CH), 123.46 (s, anil-CH), 126.20 (s, anil-CH), 127.66 (s, anil-C), 129.41 (s, Py-CH), 160.92 (br d, $^3J_{PC}$ = 11.4 Hz, Py-C), 166.9 (br s, Py-C), 169.11 (s, anil-C). Acceptable elemental analysis results for **25** could not be obtained. A copy of the NMR spectrum of **25** appears in the Supporting Information.

■ ASSOCIATED CONTENT

Ⓢ Supporting Information

Crystallographic data (CIF); figure of X-ray structure of **4**; and figures of ^{1}H and ^{31}P{^{1}H} spectra of the complexes **2**, **6**, **9**, **10**, **14**, **16**, **24**, and **25**. This material is available free of charge via the Internet at http://pubs.acs.org.

■ AUTHOR INFORMATION

Corresponding Author

*E-mail: david.milstein@weizmann.ac.il.

Notes

The authors declare no competing financial interest.

Biographies

David Milstein received his Ph.D. degree at the Hebrew University of Jerusalem in 1976 with Prof. Blum. He carried out postdoctoral studies at Colorado State University, where together with his advisor, John Stille, he discovered the Stille reaction. In 1979 he joined the DuPont Company in Wilmington, DE, where he became a Group Leader in the homogeneous catalysis area. In 1987 he accepted a professorial appointment at the Weizmann Institute of Science, where he was Head of the Department of Organic Chemistry in 1996−2005. In 2000 he became Head of the Kimmel Center for Molecular Design. He has been the Israel Matz Professor of Organic Chemistry since 1996. His research interests focus on the development of fundamental organometallic chemistry and its application to the design of new sustainable processes catalyzed by transition-metal complexes. He has served on several editorial boards, and he is a member of the German National Academy of Sciences. Awards received include the Kolthoff

Prize, the Israel Chemical Society Prize, the ACS Award in Organometallic Chemistry, the RSC Sir Geoffrey Wilkinson Award, and the Meitner-Humboldt Award; in 2012 he received the Israel Prize (Israel's highest honor).

Moran Feller received her M.S. degree for her work with Prof. Yoel Kashman in the field of natural product isolation and structural elucidation. In 2004 Moran joined the Milstein group, where she investigated the synthesis and reactivity of phosphino-pyridine pincer complexes of late transition metals. After graduating with a Ph.D. degree in 2008, Moran remained in the group as a postdoctoral fellow and in 2011 became an assistant staff scientist. Moran's research focuses on the activation of N−H and O−H bonds by phosphino-pyridine pincer complexes of late transition metals, primarily employing metal−ligand cooperation.

Yael Diskin-Posner did her M.Sc. degree with Prof. Uri Shmueli from the Tel-Aviv University. After a few years in the biotechnology industry, she returned to do a Ph.D. in crystallography at the Tel-Aviv University with Prof. Israel Goldberg, which she finished in 2003. She carried out her postdoctoral studies at the Weizmann Institute under the supervision of Prof. Zippora Shakked, working on p53-DNA binding domain structures. Since 2007 she has been a staff scientist in the chemical research support department in the Weizmann Institute of Science. She received the Levine-Jortner prize from the Israel Chemical Society in 2002.

Linda Shimon received her Ph.D. degree at the Weizmann Institute in 1988 in the department of structural chemistry. She carried out her postdoctoral studies at Harvard University, in the group of Prof. Stephen Harrison, where she worked on the crystallographic studies of protein/DNA complexes. In 1993 she returned to the Weizmann Institute to the X-ray crystallography laboratory. Since 1997 she has headed the X-ray laboratory and the Kimmelman Laboratory for Macromolecular Crystallography. She has received several awards, including the Schmidt Prize and the Maxine Singer Prize from the Weizmann Institute, and serves on the referee board for *Acta Crystallographica*.

Eyal Ben-Ari received his B.Sc. in chemistry in 1999 at Tel-Aviv University. Between the years 2000 and 2007 he conducted his M.Sc. and Ph.D. research with Prof. David Milstein, at the Weizmann Institute of Science. His research dealt with cleavage of strong C−H bonds by iridium and rhodium PNP pincer complexes. Currently he is a team leader at Agan Aroma and Fine Chemicals Co.

■ ACKNOWLEDGMENTS

This research was supported by the European Research Council under the FP7 framework, (ERC No. 246837), by the Israel Science Foundation, by the MINERVA Foundation, and by the Kimmel Center for Molecular Design. D.M. holds the Israel Matz Professorial Chair of Organic Chemistry.

■ REFERENCES

(1) For recent reviews, see: (a) Gunanathan, C.; Milstein, D. *Acc. Chem. Res.* **2011**, *44*, 588. (b) Gunanathan, C.; Milstein, D. *Top. Organomet. Chem* **2011**, *37*, 55. (c) Milstein, D. *Top. Catal* **2010**, *53*, 915. (d) van der Vlugt, J. L.; Reek, J. N. H. *Angew. Chem., Int. Ed.* **2009**, *48*, 8832.

(2) (a) Zhang, J.; Leitus, G.; Ben-David, Y.; Milstein, D. *J. Am. Chem. Soc.* **2005**, *127*, 10840. (b) Zhang, J.; Gandelman, M.; Shimon, L. J. W.; Milstein, D. *Dalton Trans.* **2007**, 107. (c) Zhang, J.; Leitus, G.; Ben-David, Y.; Milstein, D. *Angew. Chem., Int. Ed.* **2006**, *45*, 1113. (d) Gunanathan, C.; Ben-David, Y.; Milstein, D. *Science* **2007**, *317*, 790. (e) Gnanaprakasam, B.; Ben-David, Y.; Milstein, D. *Adv. Synth. Catal.* **2010**, *352*, 3169. (f) Gnanaprakasam, B.; Milstein, D. *J. Am. Chem. Soc.* **2011**, *133*, 1682. (g) Balaraman, E.; Gunanathan, C.; Zhang, J.; Shimon, L. J. W.; Milstein, D. *Nat. Chem.* **2011**, *3*, 609. (h) Zhang, J.; Balaraman, E.; Leitus, G.; Milstein, D. *Organometallics* **2011**, *30*, 5716. (i) Gnanaprakasam, B.; Balaraman, E.; Gunanathan, C.; Milstein, D. *J. Polym. Sci., Part A: Polym. Chem.* **2012**, *50*, 1755.

(3) For bipyridyl-based PNN complexes, see refs 2g and 2i and also: (a) Balaraman, E.; Gnanaprakasam, B.; Shimon, L. J. W.; Milstein, D. *J. Am. Chem. Soc.* **2010**, *132*, 16756. (b) Balaraman, E.; Ben-David, Y.; Milstein, D. *Angew. Chem., Int. Ed.* **2011**, *50*, 11702. (c) Balaraman, E.; Fogler, E.; Milstein, D. *Chem. Commun.* **2012**, *48*, 1111.

(4) (a) Zhang, J.; Gandelman, M.; Shimon, L. J. W.; Rozenberg, H.; Milstein, D. *Organometallics* **2004**, *23*, 4026. (b) Gnanaprakasam, B.; Zhang, J.; Milstein, D. *Angew. Chem., Int. Ed.* **2010**, *49*, 1468.

(5) (a) Gunanathan, C.; Gnanaprakasam, B.; Iron, M. A.; Shimon, L. J. W.; Milstein, D. *J. Am. Chem. Soc.* **2010**, *132*, 14763. (b) Gunanathan, C.; Shimon, L. J. W.; Milstein, D. *J. Am. Chem. Soc.* **2009**, *131*, 3146. (c) Gunanathan, C.; Milstein, D. *Angew. Chem., Int. Ed.* **2008**, *47*, 8661.

(6) (a) Langer, R.; Leitus, G.; Ben-David, Y.; Milstein, D. *Angew. Chem., Int. Ed.* **2011**, *50*, 2120. (b) Langer, R.; Diskin-Posner, Y.; Leitus, G.; Shimon, L. J. W.; Ben-David, Y.; Milstein, D. *Angew. Chem., Int. Ed.* **2011**, *50*, 9948. (c) Langer, R.; Iron, M. A.; Konstantinovski, L.; Diskin-Posner, Y.; Leitus, G.; Ben-David, Y.; Milstein, D. *Chem.—Eur. J.* **2012**. DOI: 10.1002/chem.201200159.

(7) Fogler, E.; Balaraman, E.; Ben-David, Y.; Leitus, G.; Shimon, L. J. W.; Milstein, D. *Organometallics* **2011**, *30*, 3826.

(8) Zeng, H.; Guan, Z. *J. Am. Chem. Soc.* **2011**, *133*, 1159.

(9) Gnanaprakasam, B.; Balaraman, E.; Ben-David, Y.; Milstein, D. *Angew. Chem., Int. Ed.* **2011**, *50*, 12240.

(10) Hunsicker, D. M.; Dauphinais, B. C.; McIlrath, S. P.; Robertson, N. J. *Macromol. Rapid Commun.* **2012**, *33*, 232.

(11) (a) Zeng, G.; Li, S. *Inorg. Chem.* **2011**, *50*, 10572. (b) Li, H.; Wang, X.; Huang, F.; Lu, G.; Jiang, J.; Wang, Z.-X. *Organometallics* **2011**, *30*, 5233. (c) Sandhya, K. S.; Suresh, C. H. *Organometallics* **2011**, *30*, 3888. (d) Cantillo, D. *Eur. J. Inorg. Chem.* **2011**, *19*, 3008. (e) Yang, X. *Inorg. Chem.* **2011**, *50*, 12836.

(12) (a) Rigoli, J. W.; Moyer, S. A.; Pearce, S. D.; Schomaker, J. M. *Org. Biomol. Chem.* **2012**, *10*, 1746. (b) He, L.-P.; Chen, T.; Xue, D.-X.; Eddaoudi, M.; Huang, K.-W. *J. Organomet. Chem.* **2012**, *700*, 202. (c) Huff, C. A.; Sanford, M. S. *J. Am. Chem. Soc.* **2011**, *133*, 18122. (d) Sun, Y.; Koehler, C.; Tan, R.; Annibale, V. T.; Song, D. *Chem. Commun.* **2011**, *47*, 8349. (e) del Pozo, C.; Iglesias, M.; Sanchez, F. *Organometallics* **2011**, *30*, 2180. (f) Staubitz, A.; Sloan, M. E.; Robertson, A. P. M.; Friedrich, A.; Schneider, S.; Gates, P. J.; Schmedt auf der Gunne, J.; Manners, I. *J. Am. Chem. Soc.* **2010**, *132*, 13332. (g) van der Vlugt, J. I.; Lutz, M.; Pidko, E. A.; Vogt, D.; Spek, A. L. *Dalton Trans.* **2009**, *6*, 1016. (h) Tanaka, R.; Yamashita, M.; Nozaki, K. *J. Am. Chem. Soc.* **2009**, *131*, 14168.

(13) (a) Ben Ari, E.; Leitus, G.; Shimon, L. J. W.; Milstein, D. *J. Am. Chem. Soc.* **2006**, *128*, 15390. (b) Schwartsburd, L.; Iron, M. A.; Konstantinovski, L.; Diskin-Posner, Y.; Leitus, G.; Shimon, L. J. W.; Milstein, D. *Organometallics* **2010**, *29*, 3817.

(14) (a) Iron, M. A.; Ben-Ari, E.; Cohen, R.; Milstein, D. *Dalton Trans.* **2009**, 9433. (b) Zeng, G.; Guo, Y.; Li, S. *Inorg. Chem.* **2009**, *48*, 10257.

(15) Schwartsburd, L.; Iron, M. A.; Konstantinovski, L.; Ben-Ari, E.; Milstein, D. *Organometallics* **2011**, *30*, 2721.

(16) Kohl, S. W.; Weiner, L.; Schwartsburd, L.; Konstantinovski, L.; Shimon, L. J. W.; Ben-David, Y.; Iron, M. A.; Milstein, D. *Science* **2009**, *324*, 74.

(17) (a) Lawrence, S. A. *Amines: Synthesis, Properties and Applications*; Cambridge University Press: Cambridge, U.K., 2004. (b) Roundhill, D. M. *Chem. Rev.* **1992**, *92*, 1.

(18) For recent reviews, see: (a) Klinkenberg, J. L.; Hartwig, J. F. *Angew. Chem., Int. Ed.* **2011**, *50*, 86. (b) van der Vlugt, J. I. *Chem. Soc. Rev.* **2010**, *39*, 2302. (c) Enthaler, S. *ChemSusChem* **2010**, *3*, 1024.

(19) (a) Müller, T. E.; Hultzsch, K. C.; Yus, M.; Foubelo, F.; Tada, M. *Chem. Rev.* **2008**, *108*, 3795. (b) Hartwig, J. F. *Pure Appl. Chem.* **2004**, *76*, 507. (c) Müller, T. E.; Beller, M. *Chem. Rev.* **1998**, *98*, 675.

(20) (a) Eilbracht, P.; Baerfacker, L.; Buss, C.; Hollmann, C.; Kitsos-Rzychon, B. E.; Kranemann, C. L.; Rische, T.; Roggenbuck, R.; Schmidt, A. *Chem. Rev.* **1999**, *99*, 3329. (b) Eilbracht, P.; Schmidt, A. M. *Top. Organomet. Chem.* **2006**, *18*, 65.
(21) For recent reviews, see: (a) Sadig, J. E. R.; Willis, M. C. *Synthesis* **2011**, *1*, 1. (b) Aubin, Y.; Fischmeister, C.; Thomas, C. M.; Jean-Luc, R. *Chem. Soc. Rev.* **2010**, *39*, 413. (c) Enthaler, S. *ChemSusChem* **2010**, *3*, 1024. (d) Gillespie, J. A.; Dodds, D. L.; Kamer, P. C. J. *Dalton Trans.* **2010**, *39*, 2751.
(22) (a) Storer, R. I.; Carrera, D. E.; Ni, Y.; MacMillan, D. W. C. *J. Am. Chem. Soc.* **2006**, *128*, 84. (b) Nugent, T. C.; El-Shazly, M. *Adv. Synth. Catal.* **2010**, *352*, 753. (c) Gomez, S.; Peters, J. A.; Maschmeyer, T. *Adv. Synth. Catal.* **2002**, *344*, 1037. (d) Kobayashi, S.; Ishitani, H. *Chem. Rev.* **1999**, *99*, 1069.
(23) Nitriles are usually reduced by stoichiometric amounts of metal hydrides or by heterogeneous catalytic hydrogenation. Few homogeneous hydrogenation catalysts based on ruthenium, iridium, nickel, and rhodium are also known. For ruthenium catalysis, see: (a) Grey, R. A.; Pez, G. P.; Wallo, A. *J. Am. Chem. Soc.* **1981**, *103*, 7536. (b) Suarez, T.; Fontal, B. *J. Mol. Catal.* **1988**, *45*, 335. (c) Mukherjee, D. K.; Palit, B. K.; Saha, C. R. *J. Mol. Catal.* **1994**, *88*, 57. (d) Takemoto, S.; Kawamura, H.; Yamada, Y.; Okada, T. *Organometallics* **2002**, *21*, 3897. (e) Enthaler, S.; Addis, D.; Junge, K.; Erre, G.; Beller, M. *Chem.—Eur. J.* **2008**, *14*, 9491. (f) Enthaler, S.; Junge, K.; Addis, D.; Erre, G.; Beller, M. *ChemSusChem* **2008**, *1*, 1006. (g) Addis, D.; Enthaler, S.; Junge, K.; Wendt, B.; Beller, M. *Tetrahedron Lett.* **2009**, *50*, 3654. For iridium catalysis, see: (h) Chin, C. S.; Lee, B. *Catal. Lett.* **1992**, *14*, 135. For nickel catalysis, see: (I) Zerecero-Silva, P.; Jimenez-Solar, I.; Crestani, M. G.; Arévalo, A.; Barrios-Francisco, R.; García, J. J. *Appl. Catal., A* **2009**, *363*, 230. For rhodium catalysis, see: (j) Yoshida, T.; Okano, T.; Otsuka, S. *J. Chem. Soc., Chem. Commun.* **1979**, 870.
(24) (a) Casalnuovo, A. L.; Calabrese, J. C.; Milstein, D. *J. Am. Chem. Soc.* **1988**, *110*, 6738. (b) Ir(I)-catalyzed asymmetric hydroamination: Dorta, R.; Egli, P.; Zucher, F.; Togni, A. *J. Am. Chem. Soc.* **1997**, *119*, 10857.
(25) Sappa, E.; Milone, L. *J. Organomet. Chem.* **1973**, *61*, 383.
(26) Ladipo, F. T.; Merola, J. S. *Inorg. Chem.* **1990**, *29*, 4172.
(27) Kanzelberger, M.; Zhang, X.; Emge, T. J.; Goldman, A. S.; Zhao, J.; Incarvito, C.; Hartwig, J. F. *J. Am. Chem. Soc.* **2003**, *125*, 13644.
(28) Cartwright Sykes, A.; White, P.; Brookhart, M. *Organometallics* **2006**, *25*, 1664.
(29) For more examples of N−H oxidative addition by late transition-metal complexes, see: (a) Hartwig, J. F.; Andersen, R. A.; Bergman, R. G. *Organometallics* **1991**, *10*, 1875. (b) Fulton, J. R.; Holland, A. W.; Fox, D. J.; Bergman, R. G. *Acc. Chem. Res.* **2002**, *35*, 44. (c) Pavlik, S.; Mereiter, K.; Schmid, R.; Kirchner, K. *Organometallics* **2003**, *22*, 1771. (d) Grotjahn, D. B.; Gong, Y.; DiPasquale, A. G.; Zakharov, L. N.; Rheingold, A. L. *Organometallics* **2006**, *25*, 5693.
(30) (a) Casalnuovo, A. L.; Calabrese, J. C.; Milstein, D. *Inorg. Chem.* **1987**, *26*, 971. (b) Koelliker, R.; Milstein, D. *Angew. Chem., Int. Ed. Engl.* **1991**, *30*, 707. (c) Schulz, M.; Milstein, D. *J. Chem. Soc., Chem. Commun.* **1993**, 318.
(31) Zhao, J.; Goldman, A. S.; Hartwig, J. F. *Science* **2005**, *307*, 1080.
(32) Huang, Z.; Zhou, J. S.; Hartwig, J. F. *J. Am. Chem. Soc.* **2010**, *132*, 11458.
(33) Morgan, E.; MacLean, D. F.; McDonald, R.; Turculet, L. *J. Am. Chem. Soc.* **2009**, *131*, 14234.
(34) Fafard, C. M.; Adhikari, D.; Foxman, B. M.; Mindiola, D. J.; Ozerov, O. V. *J. Am. Chem. Soc.* **2007**, *129*, 10318.
(35) Mena, I.; Casado, M. A.; Garcia-Orduna, P.; Polo, V.; Lahoz, F. J.; Fazal, A.; Oro, L. A. *Angew. Chem., Int. Ed.* **2011**, *50*, 11735.
(36) Khaskin, E.; Iron, M. A.; Shimon, L. J. W.; Zhang, J.; Milstein, D. *J. Am. Chem. Soc.* **2010**, *132*, 8542.
(37) Muniz, K.; Lishchynskyi, A.; Streuff, J.; Nieger, M.; Escudero-Adan, E. C.; Belmonte, M. M. *Chem. Commun.* **2011**, *47*, 4911.
(38) The ^{1}H and $^{13}C\{^{1}H\}$ NMR spectra of **1** exhibit broad signals for the amine "benzylic arm", which are sharpening upon cooling to 253 K. In addition, complex **1** exhibits two IR bands at 2069 and 2157 cm^{-1}, in line with the existence of two mononuclear dinitrogen "end-on" fluxional species. For more details, see the Supporting Information.
(39) Complex **1** reacts slowly with methylene chloride at ambient temperature to give a new unidentified complex, probably the C−Cl activation product ($\delta^{31}P\{^{1}H\}$ NMR (DCM-d_2): 65.51 (d, $^{1}J_{RhP}$ = 127.1 Hz)).
(40) See the Supporting Information.
(41) We have observed previously that a weak interaction of the counterion with the metal center may be temperature-independent and that, at lower temperatures, the cationic complex is preferred, whereas at higher temperature, the neutral complex is observed. (a) Gandelman, M.; Konstantinovski, L.; Rozenberg, H.; Milstein, D. *Chem.—Eur. J.* **2003**, *9*, 2595. (b) Feller, M.; Ben-Ari, E.; Iron, M. A.; Diskin-Posner, Y.; Leitus, G.; Shimon, L. J. W.; Konstantinovski, L.; Milstein, D. *Inorg. Chem.* **2010**, *49*, 1615.
(42) For more examples of coordinated BF_4, see: (a) Frech, C. M.; Shimon, L. J. W.; Milstein, D. *Organometallics* **2009**, *28*, 1900. (b) Majumdar, M.; Patra, S. K.; Kannan, M.; Dunbar, K. R.; Bera, J. K. *Inorg. Chem.* **2008**, *47*, 2212. (c) Drabent, K.; Clunlk, Z.; Ozarowskl, A. *Inorg. Chem.* **2008**, *47*, 3358. (d) Feller, M.; Ben-Ari, E.; Gupta, T.; Shimon, L. J. W.; Leitus, G.; Diskin- Posner, Y.; Weiner, L.; Milstein, D. *Inorg. Chem.* **2007**, *46*, 10479. (e) Salem, H.; Ben-David, Y.; Shimon, L. J. W.; Milstein, D. *Organometallics* **2006**, *25*, 2292. (f) Frech, C. M.; Milstein, D. *J. Am. Chem. Soc.* **2006**, *128*, 12434. (g) Rybtchinski, B.; Oevers, S.; Montag, M.; Vigalok, A.; Rozenberg, H.; Martin, J. M. L.; Milstein, D. *J. Am. Chem. Soc.* **2001**, *123*, 9064. (h) Beck, W.; Sunkel, K. *Chem. Rev.* **1988**, *88*, 1405. (i) Sutherland, B. R.; Cowie, M. *Inorg. Chem.* **1984**, *23*, 1290.
(43) MacKay, B. A.; Fryzuk, M. D. *Chem. Rev.* **2004**, *104*, 385.
(44) Unlike complex **1**, complex **2** does not exhibit fluxional behavior.
(45) Hermann, D.; Gandelman, M.; Rozenberg, H.; Shimon, L. J. W.; Milstein, D. *Organometallics* **2002**, *21*, 812.
(46) The ethylene signals in the ^{1}H and $^{13}C\{^{1}H\}$ NMR spectra are lacking P−H coupling, presumably because of rapid rotation. See: Cramer, R. *J. Am. Chem. Soc.* **1964**, *86*, 217.
(47) For the X-ray structure of complex **4**, see the Supporting Information.
(48) (a) The C═C bond length in free gaseous ethylene is estimated to be 1.3305(10) Å. Craig, N. C.; Groner, P.; McKean, D. C. *J. Phys. Chem. A* **2006**, *110*, 7461. (b) The C═C bond length from X-ray data is 1.313 Å. Van Nes, G. J. H.; Vos, A. *Acta Crystallogr., Sect. B* **1979**, *35*, 2593.
(49) Feller, M.; Iron, A. M.; Shimon, L. J. W.; Diskin-Posner, Y.; Leitus, G.; Milstein, D. *J. Am. Chem. Soc.* **2008**, *130*, 14374.
(50) The $^{13}C\{^{1}H\}$ NMR of a mixture of complexes **5** and **5a** gives rise to two signals at 63.04 (d, J = 1.8 Hz) and 63.47 (d, J = 1.8 Hz) assigned to the Py−CH_2−N functionality. See the Experimental Section.
(51) (a) Hanson, S. K.; Heinekey, D. M.; Goldberg, K. I. *Angew. Chem., Int. Ed.* **2007**, *46*, 4736. (b) Hanson, S. K.; Heinekey, D. M.; Goldberg, K. I. *Organometallics* **2008**, *27*, 1454.
(52) Complex **5** stands for the mixture of the monomer and the dimer complexes **5** and **5a**, respectively.
(53) (a) Tejel, C.; Ciriano, M. A.; Bordonaba, M.; López, J. A.; Lahoz, F. J.; Oro, L. A. *Inorg. Chem.* **2002**, *41*, 2348. (b) Tejel, C.; Ciriano, M. A.; Bordonaba, M.; López, J. A.; Lahoz, F. J.; Oro, L. A. *Chem.—Eur. J.* **2002**, *8*, 3128. (c) Fandos, R.; Martínez-Ripoll, M.; Otero, A.; Ruiz, M. J.; Rodríguez, A.; Terreros, P. *Organometallics* **1998**, *17*, 1465.
(54) For a concise illustration of the SST technique, see: (a) Jarek, R. L.; Flesher, R. J.; Shin, S. K. *J. Chem. Educ.* **1997**, *74*, 978. For previous examples of the use of spin saturation transfer in studies of chemical exchange, see: (b) Portnoy, M.; Milstein, D. *Organometallics* **1993**, *12*, 1665. (c) Vigalok, A.; Kraatz, H.-B.; Konstantinovski, L.; Milstein, D. *Chem.—Eur. J.* **1997**, *3*, 253. (d) Rybtchinski, B.; Konstantinovski, L.; Shimon, L. J. W.; Vigalok, A.; Milstein, D. *Chem.—Eur. J.* **2000**, *6*, 3287. (e) Montag, M.; Schwartsburd, L.;

Cohen, R.; Leitus, G.; Ben-David, Y.; Martin, J. M. L.; Milstein, D. *Angew. Chem., Int. Ed.* **2007**, *46*, 1901.
(55) Upon saturation of signal a, only the adjacent signal was affected due to the proximity to the saturated signal and not as a result of chemical exchange.
(56) All reactions were performed under the same conditions: 0.011 mmol of the complex and the aniline in 0.5 mL of THF were placed in a J. Young NMR tube, and the reactions were followed by $^{31}P\{^{1}H\}$ NMR at ambient temperature or 60 °C.
(57) The reaction of complexes **5**−**7** and **9** with an equivalent of aniline may be sluggish, due to lower stability of the anilide complexes **10** and **14**, as compared with the more electron-poor anilide complexes. Complexes **10** and **14** can be obtained selectively by addition of an excess of aniline, or by deprotonation of complexes **16** and **17**, respectively.
(58) In the case of the reaction of complexes **9**−**15** and triethylphosphine, after 4 days at ambient temperature, traces of new unidentified complexes were obtained according to $^{31}P\{^{1}H\}$ NMR.
(59) The $^{31}P\{^{1}H\}$ NMR spectrum of the reaction mixtures is similar to the spectrum that was obtained by addition of an excess of triethylphosphine to complex **5**. According to the signal pattern of the spectrum, it is likely that the reaction mixture includes complexes with two and three PEt_3 ligands.
(60) Complexes **10**, **13**, **14**, and **15** were also reacted with an excess of ethylene. In the case of complexes **10** and **13**, the reaction with ethylene was found to be nonselective and led to partial decomposition of the complexes and to the formation of unidentified precipitate. The reaction of complex **14** with ethylene led to the formation of free aniline and complex **7**. The reaction of complex **15** with ethylene resulted in the formation of a new major complex, according to the $^{31}P\{^{1}H\}$ NMR of the reaction mixture, which gives rise to a signal at 42.84 ppm (d, $^{1}J_{RhP}$ = 100.4 Hz, 90% by integration). We assume that the product is an ethylene adduct complex of **15**; however, due to its fluxionality, we could not detect the ethylene ligand. The reaction of complex **15** and ethylene was found to be reversible, and upon heating the reaction mixture to 60 °C, only complex **15** was obtained.
(61) Noyori, R.; Yamakawa, M.; Hashiguchi, S. *J. Org. Chem.* **2001**, *66*, 7931.
(62) The fact that aniline N−H activation was faster with the COE complex **9** than with the ethylene complex **7** is probably due to the lack of stability of the anilide complexes **10** and **14** as compared with the less electron-rich *p*-nitroanilide complexes **13** and **15**. Thus, the equilibrium described in pathway A is further shifted towards the anilide complexes in the case of the more loosely bound COE complex **9** than in the case of the ethylene complex **7**.
(63) The COE ligand in complex **9** is weakly bound; thus, if complex **9** in the presence of aniline is in an equilibrium of coordination/dissociation of COE/aniline, an excess of COE will push the equilibrium toward the COE-bound complex, which is the reactive species in the associative mechanism. However, such an equilibrium was not observable.
(64) (a) Vuzman, D.; Poverenov, E.; Shimon, L. J. W.; Diskin-Posner, Y.; Milstein, D. *Organometallics* **2008**, *27*, 2627. (b) Feller, M.; Ben-Ari, E.; Iron, M. A.; Diskin-Posner, Y.; Leitus, G.; Shimon, L. J. W.; Konstantinovski, L.; Milstein, D. *Inorg. Chem.* **2010**, *49*, 1615 and references therein.
(65) Jansen, A.; Pitter, S. *Monatsh. Chem.* **1999**, *130*, 783.
(66) van der Ent, A.; Onderdelinden, A. L. *Inorg. Synth.* **1990**, *28*, 90.
(67) Cramer, R. *Inorg. Synth.* **1990**, *28*, 86.

NOTE ADDED AFTER ASAP PUBLICATION

In the version of this paper published on May 18, 2012, some biographical information was inadvertently left out. The version that appears as of May 24, 2012, contains this information.